ISAS - INTERNATIONAL SCHOOL
FOR ADVANCED STUDIES

Functional diversity of voltage–dependent calcium channels in cerebellar granule neurons

Thesis submitted for the degree of

"Doctor Philosophiæ"

CANDIDATE

Lia Chiara Forti

SUPERVISOR

Prof. Daniela Pietrobon

November 1992

TRIESTE

SISSA - SCUOLA
INTERNAZIONALE
SUPERIORE
DI STUDI AVANZATI
TRIESTE
Strada Costiera 11

SISSA ISAS
SCUOLA INTERNAZIONALE SUPERIORE DI STUDI AVANZATI
INTERNATIONAL SCHOOL FOR ADVANCED STUDIES

Functional diversity of voltage–dependent calcium channels in cerebellar granule neurons

Thesis submitted for the degree of

"Doctor Philosophiæ"

CANDIDATE

Lia Chiara Forti

SUPERVISORS

Prof. Daniela Pietrobon

November 1992

Contents

PART ONE **INTRODUCTION**

1. Voltage-dependent calcium channels 1

Ca^{2+} signalling 1

Voltage sensitive calcium channels 3

L-type Ca^{2+} channels 5

N-type Ca^{2+} channels 13

P-type Ca^{2+} channels 16

About this thesis 17

PART TWO **RESULTS**

2. DHP-sensitive channels 21

Functional diversity of L-type Ca^{2+} channels 21

Unique properties of L-type channels with anomalous gating 29

Voltage-dependent equilibrium between gating modes 33

3. DHP-insensitive channels **40**

C_1 channel 40

C_2 channel 47

C_3 and C_4 channels 51

4. Discussion **56**

Appendix: Experimental procedures **62**

References **67**

Acknowledgments **77**

Part one

Introduction

Chapter 1

Voltage dependent calcium channels

Calcium signalling

Intracellular calcium signals are involved in a host of cellular functions in virtually every cell type.

Cytoplasmic calcium levels ($[Ca^{2+}]_{cyt}$) at rest range around 20-300 nM, while in the extracellular milieu the calcium concentration is about 10^4 times higher (around 2 mM), and calcium sequestered in intracellular organelles can be even higher. The low cytoplasmic calcium levels are maintained by active calcium extrusion mechanisms, namely the membrane-bound Ca^{2+}-ATPases and the Na^+/Ca^{2+} exchanger that transport internal calcium ions towards the external medium; excess cytoplasmic calcium can also be taken up by internal stores.

Many external signals reaching the cell membrane generate a transient elevation in $[Ca^{2+}]_{cyt}$, either via an influx through Ca^{2+}-permeable ionic channels or through release from internal stores following the generation of a chain of internal messengers. The elevation of cytoplasmic calcium above the resting level is the

trigger for events as diverse as hormone secretion and neurotransmitter release, muscle contraction, events related to cell motility and death, gene expression, modulation of cell excitability and modulation of synaptic strenght, neuronal migration and growth, and many others. Calcium ions trigger so many cellular events by binding to various Ca^{2+}-binding proteins, which in turn generate a cascade of further effects.

The ability of a given $[Ca^{2+}]_{cyt}$ elevation to generate a specific cellular response depends on many factors.

First of all, the Ca^{2+}-binding proteins have variable affinities. To give some examples, calmodulin, troponin and related proteins, involved in activation of various enzymes controlling e.g. cyclic nucleotides metabolism and protein phosphorylation, are very sensitive to $[Ca^{2+}]$ changes between 0.1 and 10 μM. Intracellular Ca^{2+} ions also directly regulate cell excitability acting on membrane channels: some K^+ and Cl^- channels are activated or modulated by 100-900 nM Ca^{2+}, while 1 to 6 μM Ca^{2+} activates a non-specific monovalent cation channel. The Ca^{2+}-binding protein(s) mediating neurotransmitter release is still unknown, however it seems that near specialized synaptic membrane areas where release takes place $[Ca^{2+}]$ can rise transiently up to 1 mM, increasing locally by 4 orders of magnitude (Hille, 1992); this suggests that the Ca^{2+} affinity of the unknown protein might be very low. Thus different calcium concentrations are needed to activate each specific function.

Moreover, the molecular machinery controlling a specific cell function may be confined to a given portion of the cell. The Ca^{2+}-binding proteins may be free cytoplasmic proteins or may be anchored to cellular structures (cytoskeleton, membrane) with a differential distribution in various parts of the cell. Calcium-buffering systems may compete with the target Ca^{2+}-binding proteins and lower the number of free Ca^{2+} ions reaching the target after entering the cytoplasmic region; this competition may be more or less relevant to the cell response depending on the distance between target proteins and the structures permitting calcium influx. In such cases, the local Ca^{2+} concentration around the target, and not just the global one, determines whether the cell response will take place or not.

It is then easy to conclude that cells must have the possibility to finely regulate their calcium influxes, so that the spatio-temporal patterns of Ca^{2+} gradients are appropriate to their needs. Calcium influxes can contribute also to the electrical activity of cells, namely to the generation of action potentials in cardiac cells, smooth muscle cells, and neurons.

Calcium-permeable ionic channels are a major pathway for calcium influxes. Cells have developed a number of different Ca^{2+} channels: i) voltage-dependent calcium channels, activated by changes in membrane potential; ii) channels opened after binding of an external transmitter molecule to a plasma membrane receptor in the same molecular complex as the channel (receptor-operated channels); iii) channels opened after activation of intracellular second messengers (second messenger-operated channels).
Voltage-dependent calcium channels have the highest selectivity for calcium, and are a very composite family, with an ever increasing number of identified members, differing in pharmacology and/or in kinetic properties. Following the first cloning of one of the subunits of the skeletal muscle calcium channel, many structurally different genes encoding for Ca^{2+} channel subunits have been sequenced, and work is in progress to connect these structural data with the functional behaviour of the corresponding channels.

Voltage-dependent calcium channels

Calcium channels are transmembrane proteins that, when in an open conformation, admit a passive flux of calcium ions across the membrane down their electrochemical gradient.
For the class of voltage-dependent calcium channels, the transition from closed to open conformational states is influenced by the transmembrane electrical potential. Voltage-dependent calcium channels have been found in many types of excitable and non-excitable cells. Neurons seem to be the cell type that can have

the highest number of different types in a same cell.

The first common subdivision of voltage-dependent calcium channels is based on a functional criterion: two classes of channels are distinguished by their different activation properties, the high voltage-activated (HVA) channels and the low voltage activated (LVA) channels. LVA channels activate at relatively negative potentials; they become steadily inactivated even with a small depolarization, while HVA channels activate at more positive potentials, and have variable inactivation properties. LVA channels are less characterized than HVA channels with respect to pharmacological and molecular properties.

The rest of this introduction will concentrate on HVA channels, and will give a very short account of the cellular distribution and the molecular, pharmacological, and basic single channel properties of known HVA channels. The important field of Ca^{2+} channel modulation will not be dealt with here, as it is not directly connected to the results reported in this thesis.

General discussions about Ca^{2+} channels are found in many reviews (Miller, 1987; Tsien et al., 1988; Bean, 1989; Hess, 1990; Pietrobon et al., 1990; Tsien et al., 1991; Miller, 1992; Snutch and Reiner, 1992).

HVA channels may be subdivided according to their different pharmacological properties in the following classes:

i) L-type HVA Ca^{2+} channels, sensitive to 1,4-dihydropyridine (DHP) agonists and antagonists;

ii) N-type HVA Ca^{2+} channels, sensitive to the toxin omega-conotoxin GVIA from the marine snail *Conus geographus*;

iii) P-type HVA Ca^{2+} channels, specifically sensitive to some fractions of the venom of the spider *Agelenopsis aperta*;

iv) still other not named HVA channels have no known specific inhibitors, and have been revealed up to now just by measurements of whole cell currents: they carry the portion of current that is left after administration of the drugs and toxins that block the first three classes of channels.

Virtually all of these pharmacological types include more than one channel as defined on the basis of functional and structural characteristics. This is clearly revealed by single channel patch-clamp recordings and by molecular biology studies.

L-type calcium channels

The channels of the DHP-sensitive class are identified by the presence on the channel molecule of high-affinity binding sites for 1,4-dihydropyridines, phenylalkylamines and benzothiazepines. L-type channels are found in virtually all excitable tissues and many non-excitable tissues. In some cases, a physiological role has been assigned with certainty to L-type channels: in cardiac and smooth muscle, e.g.,they are the major path for voltage-gated calcium entry and have a fundamental role in excitation-contraction coupling; in secretory cells they have been proved to participate to the regulation of hormone secretion.

The DHP ligands have been used to purify the DHP receptor from T-tubular membranes of skeletal muscle, where it is found at a very high density. This receptor consists of a 1:1:1:1 complex of four polypeptide chains, named α_1, α_2-δ, ß, and γ (see Campbell et al., 1988; Catterall et al., 1988). cDNAs for all of the subunits of the skeletal muscle DHP receptor have been cloned and sequenced (Tanabe et al., 1987, Ellis et al., 1988; Ruth et al., 1989; Jay et al., 1990). A δ subunit can be released from the α_2-δ complex upon reduction of disulfide bonds: the α_2 and δ polypeptides are derived from the same gene, proteolitically cleaved in vivo, and in the final channel complex they are disulfide bond-linked (De Jongh et al., 1990, Jay et al., 1991).
The α_2 subunit (145 KDa), the δ subunit (24-27 KDa) and the γ subunit (30 KDa) are intrinsic glycoproteins. The ß subunit (54 KDa) is a substrate for various protein kinases and lacks hydrophobicity, and it is then believed to attach noncovalently to the cytoplasmic side of α_1 (Takahashi, 1987). The α_1 subunit (175 KDa) contains the DHP binding site, multiple phosphorilation sites, and the pattern of hydrophobic

transmembrane segments which has been found also in other voltage-sensitive ion channels. This typical structure has four repeated homologous domains with six membrane spanning segments, as derived from hydropathy profiles, with segment 4, bearing 5 or 6 Arg or Lys charged residues every third position, held as a good candidate for the voltage-sensing region of the channel (Hess, 1990). Cytoplasmic segments of α_1 responsible for DHP binding (Regulla et al., 1991) and for excitation-contraction coupling in skeletal muscle (Tanabe et al., 1990) have been identified. The α_1 subunit is then an essential part of the channel, and it is able to form the channel pore itself. In fact, expression in a fibroblastic cell line of the skeletal muscle α_1 subunit alone resulted in a calcium channel activity (Peres-Reyes et al., 1989).

After the report of the primary sequence of the skeletal α_1 subunit, cDNAs for α_1 from various other tissues, including heart (Mikami et al., 1989), lung (Biel et al., 1990), vascular smooth muscle (Koch et al., 1990) and brain (see Snutch and Reiner, 1992, and Williams et al., 1992b) have been sequenced. The highly homologous heart and smooth muscle α_1 subunits are generated from the same gene by alternative splicing (Koch et al., 1990) and they both share about 70% homology with the skeletal muscle α_1 subunit. They direct the expression of a DHP-sensitive Ca^{2+} channel activity.

In brain, four different classes (A,B,C and D) of α_1 subunit cDNAs have been isolated on the basis of distinct hybridization patterns to rat brain mRNAs (Snutch et al., 1990). The four classes probably represent distinct genes or gene families, and within each class multiple isoforms are found, sometimes as a result of alternative splicing (Snutch et al., 1991; Mori et al., 1991; Perez-Reyes et al., 1990; Williams et al., 1992a,b).

The C and D proteins share 70-76% amino acid identity, while they have only 33-44% identity to the class A and B proteins. The class C subunits are almost identical to the α_1 subunit of the cardiac muscle calcium channel. While class A and class B α_1 subunits are part of DHP-insensitive channels (Mori et al., 1991; Williams et al., 1992b), both classes C and D encode for the α_1 subunit of a DHP-sensitive channel (Snutch et al., 1991, Williams et al., 1992a). Remarkably,

class C and D proteins are coexpressed in several cell lines. The channel expressed in oocytes from α_1 class D cDNA differs from the class C channels (as studied in non-neuronal tissues) in its whole-cell current–voltage relation and its partial and reversible block by 10-15 μM omega-conotoxin GVIA (Williams et al., 1992a).

Functional expression in oocytes of the brain class D α_1 subunit required coexpression of a ß subunit, while expression of α_1 subunit alone was obtained from the cardiac (Mikami et al., 1989) and smooth muscle clones (Biel et al., 1990; Koch et al., 1990). Expression of brain class C α_1 subunit has not yet been obtained. The properties of the calcium currents carried by α_1 subunits alone are different from those of calcium currents in the native tissues. This seems to depend on the lack of the regulatory effects on channel gating exerted by the other subunits (Snutch and Reiner, 1992).

If one considers that not only for the α_1 subunit, but also for the other subunits forming a calcium channel, a variety of genes and/or isoforms seems to exist (Miller, 1992), a great functional variability among each class of HVA channels can be expected.

For DHP-sensitive channels, this variability is confirmed by some electrophysiological studies. In fact, the literature reports that L-type Ca^{2+} channels from cardiac myocytes and from some peripheral neurons and secretory cells share similar functional properties, while the skeletal muscle L-type channel differs markedly from them (Pietrobon et al., 1990), and a novel type of functional behaviour has also been recently described for L-type channels in adrenal chromaffin cells (see below).

The cardiac Ca^{2+} channel is the best characterized at the whole-cell and single channel level. Single channel conductance is 20-25 pS with Ba^{2+} (100 mM) and 7-8 pS with Ca^{2+} (100 mM) as charge carriers, respectively (Reuter et al., 1982; Hess et al., 1986). Activity is characterized by clusters of bursts of openings of short duration (mean open time 1 msec), separated by long periods (tens of milliseconds to several seconds) of inactivity (Hess et al., 1984; Cavalie' et al., 1986). Dihydropyridine agonists greatly prolong the mean open time of the channel, while

dihydropyridine antagonists as nifedipine and nitrendipine are potent blockers (Hess et al., 1984; Kokubun and Reuter, 1984). The action of DHP antagonists is however voltage dependent, and the inhibition of the Ca^{2+} current increases with increasing holding potentials (Bean, 1984; Sanguinetti and Kass, 1984). With low concentrations [1] of the charge carriers Ba^{2+} or Ca^{2+} and with whole cell recordings, the Ca^{2+} current activates above -30/-20 mV, with time constants of the order of a millisecond (Reuter et al., 1982). Steady state inactivation appears with holding potentials positive to -30 or -40 mV (Sanguinetti and Kass, 1984). Inactivation develops in hundreds of milliseconds with Ba^{2+} as charge carrier (Kass and Sanguinetti, 1984), but there can be a great variability from cell to cell (Cavalie' et al., 1986). In addition to voltage-dependent inactivation, L-type channels are also subject to Ca^{2+}-dependent inactivation (Eckert and Chad, 1984). When Ca^{2+} ions are used as charge carriers, in cardiac and smooth muscle inactivation is rapid, with time constants of 20-100 ms (Kass and Sanguinetti, 1984).

L-type calcium channels in mammalian cardiac cells present some peculiar gating properties. In single channel recordings it has been observed that the typical gating with bursts of fast openings of 1 msec mean open time is sometimes interrupted by long openings with mean open times about one order of magnitude higher. These long openings appear clustered in very high open probability (p_o) episodes. High-p_o episodes are a very rare event in normal conditions (i.e. when a test depolarization

---

[1] While whole-cell studies on calcium current are usually made with a low concentration (< 10 mM) of divalent cations as charge carriers through the channels, most of the single channel studies on HVA channels have been performed using a high (90-110 mM) Ba^{2+} concentration as charge carrier in the patch pipette. This is due to the fact that the single channel conductance is always higher with Ba^{2+} than with Ca^{2+}. A physiological (2-5 mM) [Ca^{2+}] in the pipette would give almost unresolvable single channel currents. High concentrations of divalent ions have however an important consequence: for almost all voltage-dependent channels, the dependence on membrane potential of their properties is shifted along the voltage axis by changes in the concentration of divalents, in the sense of a positive shift or a negative shift for raised or lowered concentrations respectively (Hille, 1992). In the case of HVA channels, a change of [Ba^{2+}] on the external face of the membrane from 10 mM to 90-110 mM shifts activation properties about 25 mV in the positive direction (Pietrobon and Hess, 1990).

is delivered from a negative holding potential and no drugs are applied). But increasing the frequency of such high-p_o bursts of activity might represent a physiologically useful mechanism facilitating calcium influx. This hypothesis explains the interest in the study of the kinetic events underlying long openings.

In the presence of DHP agonists, most of the cardiac L-type channel openings are greatly prolonged, while in the presence of DHP antagonists the channel is often silent during depolarization. A study of single channel gating in the presence of DHPs induced Hess et al. (1984) to formulate a kinetic model of channel activity based on the concept of gating modes. A mode is by definition a set of conformational states such that transitions of the channel protein among states within the mode are much more probable than transitions out of, or into, the mode. Hess and coworkers (1984) described three modes of activity for the L-type channel, mode 0, where the channel is unable to open, mode 1, where channel openings and closings are very fast and give rise to the normal fast gating (0.5-1 msec mean open time), and mode 2, where the channel opens with long openings (10-20 msec mean open time). They reported that the effect of DHP agonists was to increase time spent by the channel in mode 2, and the effect of antagonists was to increase time spent in mode 0, while the mean open times of openings belonging to mode 1 or mode 2 after drug application were not changed with respect to control values. In other words, the action of drugs was effective only in changing the rate constants of interconversion between modes.

Following this first report the action of DHPs on the channel has been debated and alternative kinetic models of channel gating have been proposed. One objection to the mode model is based on the observation that the effect of DHP agonists on the mean open time of long openings is graded with agonist concentration (Lacerda and Brown, 1989). But while the real mechanisms of action of DHP drugs on channel gating is still unclear, it is now undoubted that long openings appearing in clusters are an intrinsic gating property of cardiac L-type channels, and thus the mode description is qualitatively a useful kinetic model for these channels.

The probability of long openings in cardiac cells has been found to increase following i) predepolarization to very positive potentials (Pietrobon and Hess, 1990),

and ii) ß-adrenergic stimulation (Yue et al., 1990). In all cases, an increase in the rate of appearence of mode 2 long openings without changes in gating within each mode was reported.

In the study of Pietrobon and Hess (1990), predepolarizations (prepulses) have been observed to be the more effective in inducing mode 2 activity the more they are prolonged and/or intense. After a prepulse, the long openings episode at the test potential is the more prolonged the more positive is the test potential. These properties have been explained with a kinetic model where mode 1 and 2 are connected with voltage-dependent first order kinetic constants, k_f and k_b, where k_f raises, and k_b diminishes with depolarization. The voltage dependence of these constants has been measured, and it was proposed that the long duration of the cardiac action potential and the voltage range of the action potential plateau should permit a shift of a significant number of L-type channels to the high-$p_o$mode. Whether this voltage-dependent facilitation of cardiac channels consists purely in a voltage-induced conformational change in the channel, or other intermediate molecules exist that sense the voltage changes, it is not known.

ß-adrenergic agonists, as isoproterenol, or membrane permeant analogues of cAMP as 8-bromo-cAMP, can also increase the frequency of transitions to the high-po mode, indicating that phosphorylation can shift the equilibrium between modes. In smooth muscle cells a similar effect of hormonal modulation has been reported (Bonev and Isenberg, 1992).

Facilitation of whole-cell calcium currents following a positive prepulse has been known for many years in adrenal chromaffin cells (Fenwick et al., 1982). A systematic investigation of the phenomenon has described the dependence of whole-cell calcium currents on prepulse intensity and duration and on test pulse potential, as well as the facilitating effect of repetitive stimuli similar to a train of action potentials (Hoshi et al., 1984).

In recent times (Artalejo et al., 1991) the calcium channels responsible for facilitation in chromaffin cells were identified as DHP-sensitive channels. These

channels have the peculiar property that they are normally quiescent with unfrequent depolarizations to potentials that strongly activate the cardiac L-type channel (-20 mV to +30 mV), and are activated only by strong predepolarizations or by repetitive depolarizations to physiological potentials. The latter kinds of stimulation change the channel activity from a very low-p_o one, with rare sparse fast openings, to a very high-p_o one, with long openings similar to those induced in the cardiac L-type channel by prepulses. The activation of these facilitation calcium channels is under biochemical as well as electrical control. One way of recruiting facilitation involves activation of intracellular protein kinase A (PKA) through stimulation with dopamine (Artalejo et al., 1990). The electrical recruitment of facilitation acts instead in a different way, involving phosphorylation of the channel or of a closely associated regulatory protein by a kinase different from PKA or from a Ca^{2+}-dependent kinase; the process does not require activity of G-proteins (Artalejo et al., 1992). The identity of the kinase responsible for voltage-dependent facilitation in these cells is still unknown. Ca^{2+} channel facilitation in chromaffin cells is thought to be important for the fast increase of the secretory response after a strong afferent stimulation.

In many central nervous system neurons L-type Ca^{2+} channels contribute only a fraction of the high-threshold whole cell Ca^{2+} current, most of which is carried by different types of DHP-insensitive Ca^{2+} channels (Regan et al., 1991; Mogul and Fox, 1991). The mixed population of voltage-dependent Ca^{2+} channel subtypes in any individual neuronal cell makes the definition of the functional properties of brain L-type channels difficult.

A variety of physiological roles has been proposed for neuronal L-type channels. Concerning neurotransmission, it is likely that L-type channels do not have a role in triggering transmitter release from many synapses: a differential effect of DHP antagonists on measured Ca^{2+} influxes and on transmitter release was in effect one of the first indirect evidences suggesting the existence of other types of calcium channels beside DHP-sensitive channels (reviewed in Miller, 1987). Experiments measuring evoked transmitter release from rat brain synaptosomes in most cases find

that release is insensitive to DHPs, presumably reflecting the fact that Ca^{2+} channels in brain nerve terminals are not L-type (Miller, 1987). Release of noradrenaline from sympathetic neurons of the superior cervical ganglion is also insensitive to DHP antagonists (Hirning et al., 1988). However, the release of substance P from cultured neurons of the dorsal root ganglia (DRG) is very sensitive to modulation by DHPs (Perney et al., 1986; Rane et al., 1987). Thus it appears that in some cases an L-channel-dependent release exists. It has been proposed that L-type Ca^{2+} channels may have a role in secretion of large, dense-core vescicles, while other channels may contribute to release of small, clear-cored vescicles (Hirning et al., 1988).

In some endocrine cells there are evidences that secretion is inhibited by DHP antagonists, as in pituitary cell lines (Reisine, 1990), in adrenal cells (Fakunding and Catt, 1980), in pancreatic ß-cells (Malaisse-Lagae et al., 1984). Thus some L-type channels may regulate hormone secretion in neurosecretory cells (Miller, 1992). This is also supported by the localization, in the central nervous system, of the mRNA encoding for a class D α_1 subunit. By in situ hybridization and by immunohistochemical techniques it was found that this mRNA is preferentially, but not exclusively, located in brain areas related to neuroendocrine and olfactory functions (Chin et al., 1992).

Several evidences suggest that L channels may not play a central role in nerve terminals and may be preferentially located in the cell soma (Miller, 1987). In a recent study using immunostaining with monoclonal antibodies specific for the α_2 subunit of the skeletal muscle DHP-sensitive channel, the stained channels appear preferentially distributed at the site where major dendrites originate from the soma (Ahlijanian et al., 1990). This happens in hippocampus, cerebral cortex, spinal cord, retina and in cerebellar Purkinje cells. The staining appears to be specific for some types of DHP-sensitive channel, as 63% of the channels labeled with [^{3}H]PN200-110 (a dihydropyridine) are immunoprecipitated while only 6% of labeled omega-Cgtx binding sites are. The location on the soma at the base of major dendrites suggests an important role of these channels in regulating the calcium concentration in the cell soma and in initiating calcium-dependent

regulatory processes. No informations are available on the electrophysiological properties of the stained channels, nor on their relation with the classes of L-type calcium channel genes found with molecular biology studies.
Other roles that have been proposed for the L-type channels in the nervous system include i) the generation of the postsynaptic calcium influx that should mediate establishment of LTP in the mossy fibers to CA3 synapses in the hippocampus (Johnston et al., 1992); ii) an involvement in heterosynaptic long term depression (Wickens and Abraham, 1991) and in some forms of NMDA-independent long term potentiation in the hippocampus (Grover and Teyler, 1990; Aniksztejn and Ben Ari, 1991); iii) in cultured cortical neurons, L-type channels have a crucial role in coupling synaptic excitation to activation of transcription factor genes and thus in regulation of gene expression and in neuronal plasticity (Murphy et al., 1991).

N-type calcium channels

N-type channels are a class of HVA channels defined by sensitivity of channel activity to the toxin omega-Conotoxin GVIA from the marine snail *Conus geographus*, and insensitivity to DHP drugs. They seem to be expressed prevalently in neuronal and neuroendocrine cells.
Histochemical localization of N-type calcium channels through autoradiographic mapping of omega-conotoxin binding sites in mammalian brain (Kerr et al., 1988; Maeda et al., 1989; Takemura et al., 1987, 1988) shows preferential binding in regions rich in synaptic connections. In the cerebellum, high marking is seen in the molecular layer, in correspondence to synapses of granule cells onto dendrites of Purkinj e neurons. The toxin receptors are probably found on granule cells parallel fibers (Maeda et al., 1989), but one report finds a reactivity to an anti-omega-conotoxin antibody also in Purkinj e cells (Fortier et al., 1991). In frog neuromuscular junction, omega-conotoxin binding sites have been localized in correspondence to active zones of the presynaptic membrane (Torri-Tarelli et al., 1990; Robitaille et al., 1990; Cohen et al., 1991), and in the hippocampus they have been localized to synaptic contact sites (Jones et al., 1989).

N-type channels give a very different contribution to the total calcium current in different neuronal types (Regan et al., 1991). In mammals (rat), they are the prevalent pathway for calcium influx in sympathetic neurons from the superior cervical ganglion; they carry about 50% of the total calcium current in sensory neurons from the dorsal root ganglion (DRG) and in spinal cord neurons, about 40% of the current in visual cortex, 27% in hippocampal neurons, while in cerebellar Purkinje cells they are almost absent: only 7% of total current is inhibited by omega-conotoxin (Regan et al., 1991). In avians (chick) the distribution of N-type channels might be different, as in chick DRG neurons omega-conotoxin inhibits from 90% to almost 100% of the total current (Aosaki and Kasai, 1989).

Concerning neurotransmission, a different role of N-type channels in avians and mammals is suggested by the fact that omega-conotoxin blocks potently Ca^{2+} uptake in chick brain synaptosomes, while the toxin has only a partial effect or no effect at all in rat brain synaptosomes (Mintz et al., 1992b). Synaptic transmission is abolished by omega-conotoxin at frog neuromuscular junction (Kerr and Yoshikami, 1984), and noradrenaline release is abolished by the toxin in rat sympathetic neurons (Hirning et al., 1988). Some synapses in mammals were found to be sensitive to the toxin, and some others not (Kamiya et al., 1988; Anderson and Harvey, 1987; Seabrook and Adams, 1989). The above data support the hypothesis of a role of N-type channels in triggering transmitter release in some but not all synapses, with species-dependent differences.

Recently, the functional expression in Xenopus oocytes of an omega-conotoxin sensitive calcium channel composed of one of the isoforms of rat brain class B α_1 subunit (see the section on DHP-sensitive channels) and of an α_2 and a ß subunit was obtained (Williams et al., 1992b). The presence of the ß subunit was necessary for channel expression, while the α_2 subunit increased the magnitude of the functional response. The class B α_1 subunit is then the pore-forming subunit of an N-type channel. The existence of multiple isoforms of the class B α_1 subunit, together with the heterogeneity of genes and isoforms coding for α_2 and ß subunits, suggests the existence of multiple, functionally different N-type channels.

The biophysical characterization of N-type channels reveals very variable whole-cell

properties. The channels are high-voltage activated with activation threshold that varies, in low divalents solutions, in the range -30 to -10 mV. Either steady-state inactivation or transient inactivation properties vary markedly in different neuronal types: N-type channels in many cells have been found to inactivate completely at holding potentials positive to -40 mV and to require negative holding potentials (<-100 mV) to reprime completely after inactivation (Fox et al., 1987a,b; Plummer et al., 1989; Jones and Marks, 1989; Aosaki and Kasai, 1989). Until recent findings, holding potential sensitivity in the range -100 to -40 mV was considered a property common to all N-type channels. However, it has been shown that in a neuroblastoma-glioma cell line (NG-108), N-type steady-state inactivation requires much more positive holding potentials (Kasai and Neher, 1992), and in adrenal chromaffin cells, an omega-conotoxin sensitive channel is unaffected by holding potential variations in the range -120 to -50 mV (Artalejo et al., 1992a; Bossu et al., 1991a). Inactivation kinetics during a depolarization can be fast, taking a few tens of milliseconds as in chick sensory neurons (Fox et al., 1987a; but see Aosaki and Kasai, 1989, that report in the same cells the existence of an N-type channel with much slower inactivation), or a few hundreds of milliseconds, with non-inactivating or much slower inactivating components, as in PC12 cells and sympathetic neurons (Plummer et al., 1989).
N-type currents in NG-108 cells (Kasai and Neher, 1992) also show a slow decay during depolarization (hundreds of milliseconds or more).

Single channel recordings of N-type Ca^{2+} channels have been reported in chick embryonic DRG neurons (Fox et al., 1987b; Aosaki and Kasai, 1989), in sympathetic neurons and PC12 cells (Plummer et al.,1989), and in adrenal chromaffin cells (Artalejo et al., 1992a; Bossu et al., 1991b), with single channel conductance varying between 13 and 20 pS with 90-110 mM Ba^{2+} as charge carrier.

P-type calcium channels

P-type channels are the predominant class of calcium channels in cerebellar Purkinje cells. The first proposal of the existence of a new class of HVA channels was made on the basis of the observation that calcium-based, high-threshold dendritic spikes in Purkinje cells were inhibited by a low-molecular (200-400 Da) weight polyamine (FTX) extracted from the crude venom of a funnel web spider, *Agelenopsis aperta* (Llinas et al., 1989). The specificity of FTX for a new class of HVA channels, not including L- and N-type channels, was however not proved. Later, a careful analysis of the pharmacological sensitivities of calcium currents in several neuronal cell types (Regan et al., 1991) proved that DHP-sensitive and omega-conotoxin-sensitive components contribute only a fraction of the total calcium current that varies from cell to cell, and remarkably in cerebellar Purkinje cells the resistant component was more than 90%, thus confirming the hypothesis of a new type of channels highly expressed in those cells. A 48 amino-acids-peptide component of the venom of *Agelenopsis aperta*, omega-Aga-IVA, was isolated and specifically proved to be ineffective on L- and N-type channels, and to inhibit 85% to 100% of the calcium current in cerebellar Purkinje neurons (Mintz et al., 1992a,b).

The current carried by P-type channels activates around -50/-40 mV, inactivates very slowly (seconds) during a depolarization, and steady state inactivation is complete at relatively positive (-20 mV) holding potentials (Regan, 1991). Only preliminary reports are available on single P-type channel properties in intact Purkinje neurons, indicating three distinct single channel conductances (Usowicz et al., 1991).

Oocyte expression of two isoforms of brain class A α_1 subunit, found to be highly expressed in cerebellum, together with α_2 and β subunits from skeletal muscle calcium channel, has produced a calcium current insensitive to nifedipine block and to omega-conotoxin block, but inhibited by crude funnel web spider venom (Mori et al., 1991), suggesting the implication of the class A α_1 subunits in forming a P-type channel.

Pharmacological experiments with the toxin omega-Aga IVA on whole cell calcium currents from different mammal neuronal tissues (Mintz et al., 1992a) and experiments with anti-FTX antibody binding (Hillman et al., 1991) have proved that P-type channels, beside being the dominant type of channel in Purkinje cells, are also widely distributed in the nervous system. The contribution to total calcium currents is variable from 10 to 50% (and is almost zero in sympathetic neurons), but probably whole cell measurements underestimate the contribution of P-type channels in nerve terminals of mammals, as is suggested by omega-Aga-IVA block of 70-80% of rat brain synaptosomal Ca^{2+} entry (Mintz et al., 1992b). Ca^{2+} currents expressed in Xenopus oocytes after injection of total rat brain mRNA were also largely (70%) blocked by FTX (Lin et al., 1990), and significantly resistant to dihydropyridine- and omega-conotoxin-block (Leonard et al., 1987). In the peripheral nervous system, FTX has been proved to block transmission at the mammalian neuromuscular junction (Uchitel et al., 1992).

Still other components of the whole-cell HVA calcium current have been found that are insensitive to the L-, N-, and P-type blockers (Regan et al., 1991; Mintz et al., 1992a), with a variable contribution in different neuronal types. Thus other types of HVA channels might be described in the future.

About this thesis

The work presented in this thesis develops in two directions.

i) As has been introduced in the first chapter, several types of voltage-dependent calcium channels exist, distinguished by their pharmacological properties, their molecular structure and their functional behaviour.

The pharmacological separation of macroscopic calcium currents has distinguished up to now a few different classes of channels (some of which preferentially located in the nervous system). However, the whole-cell study of calcium currents has revealed that a pharmacological component of the current can behave differently in different cell types, suggesting a functional diversity of channels within each class.

On the other hand, molecular biology studies have assessed the existence of a potentially enormous variety of different molecules, if one takes into account the number of possible combinations that arises from several genes or transcripts for each of the four subunits ($\alpha_1, \alpha_2 - \delta, \beta$ and γ) composing calcium channels. It is not known however how many combinations are effectively expressed in cells and/or correspond to channels with a true functional diversity, and it is unlikely that studies of reconstituted channels in expression systems might clarify exhaustively this point.

The fine regulation of internal calcium levels is of crucial relevance to intracellular signalling. Despite the great interest in understanding how a cell regulates its calcium influxes, detailed information on the types and functional characteristics of calcium channels expressed in neurons are only starting to be accumulated.

One aim of this work has been to give a contribution to this characterization. Single–channel elementary properties have been studied of voltage–dependent calcium channels in cerebellar granule cells in primary culture, using the patch–clamp technique in the cell–attached configuration (Hamill et al., 1981). Primary cultures from 8–day old rat cerebella yield a highly homogeneous population of granule cells (see Experimental Procedures). This preparation is then interesting for studying the different types of calcium channels that can be expressed in one cell type.

ii) The second subject studied in this work concerns the voltage–dependent facilitation of L–type calcium channels.

In a preceding section of this introduction it has been reported that in cardiac cells and in some endocrine cells a potentiation of the current carried by L–type channels is induced by a preceding membrane depolarization. In neurons, several types of plasticity phenomena induced by membrane activity and dependent on calcium influxes have been reported. While some long–term modification of synaptic responses are triggered by calcium influxes through NMDA–receptor–associated channels, it has been proposed that other non–NMDA–dependent plasticity phenomena need voltage–dependent calcium channels to develop.

We studied the behaviour of L–type channels in cerebellar granules with single channel recordings. Of particular interest to us was to assess if the

dependence on voltage of the facilitation kinetics could suggest a role of these channels in plasticity phenomena.

Part two

Results

Chapter 2

DHP-sensitive channels

Functional diversity of L-type Ca^{2+} channels

A defining characteristic of L- type Ca^{2+} channels is sensitivity to 1,4-dihydropyridine (DHP) agonists and antagonists. Figure 1A shows single channel currents of an L-type channel in a cerebellar granule cell before and after addition of the DHP agonist (+)-(S)-202-791. The typical greatly prolonged openings in the presence of DHP agonist (mean open time around 9 msec at +10 mV, cf Figure 5B) are similar to those previously reported for L-type channels in non neuronal (Hess et al., 1984; Kokubun and Reuter, 1984) as well as neuronal cells (Nowycky et al., 1985; Plummer et al., 1989). The rapid gating pattern in the representative control traces of Figure 1A, with bursts of brief and incompletely resolved openings (the so called mode 1) interrupted by rare periods of activity with much longer open durations (the so called mode 2), is similar to that reported for cardiac L-type channels (Hess et al., 1984; Pietrobon and Hess, 1990). The main distinctive features with respect to the cardiac channels are: i) the shorter durations of openings (Figure 2A, see legend) and ii) the presence of frequent transitions to a slightly lower subconductance level during mode 2 (see first trace in Figure 1A, and Figure 2B). The average single channel conductance of cerebellar L-type channels with gating similar to that in Figure 1A was 27.4 ± 0.65 pS (n=5, with i=1.63 ± 0.035 pA at 0 mV). The average single channel conductance of the subconductance level was 23.1 ± 0.19 pS (n=3, with i= 1.26 ± 0.025 pA at 0 mV).

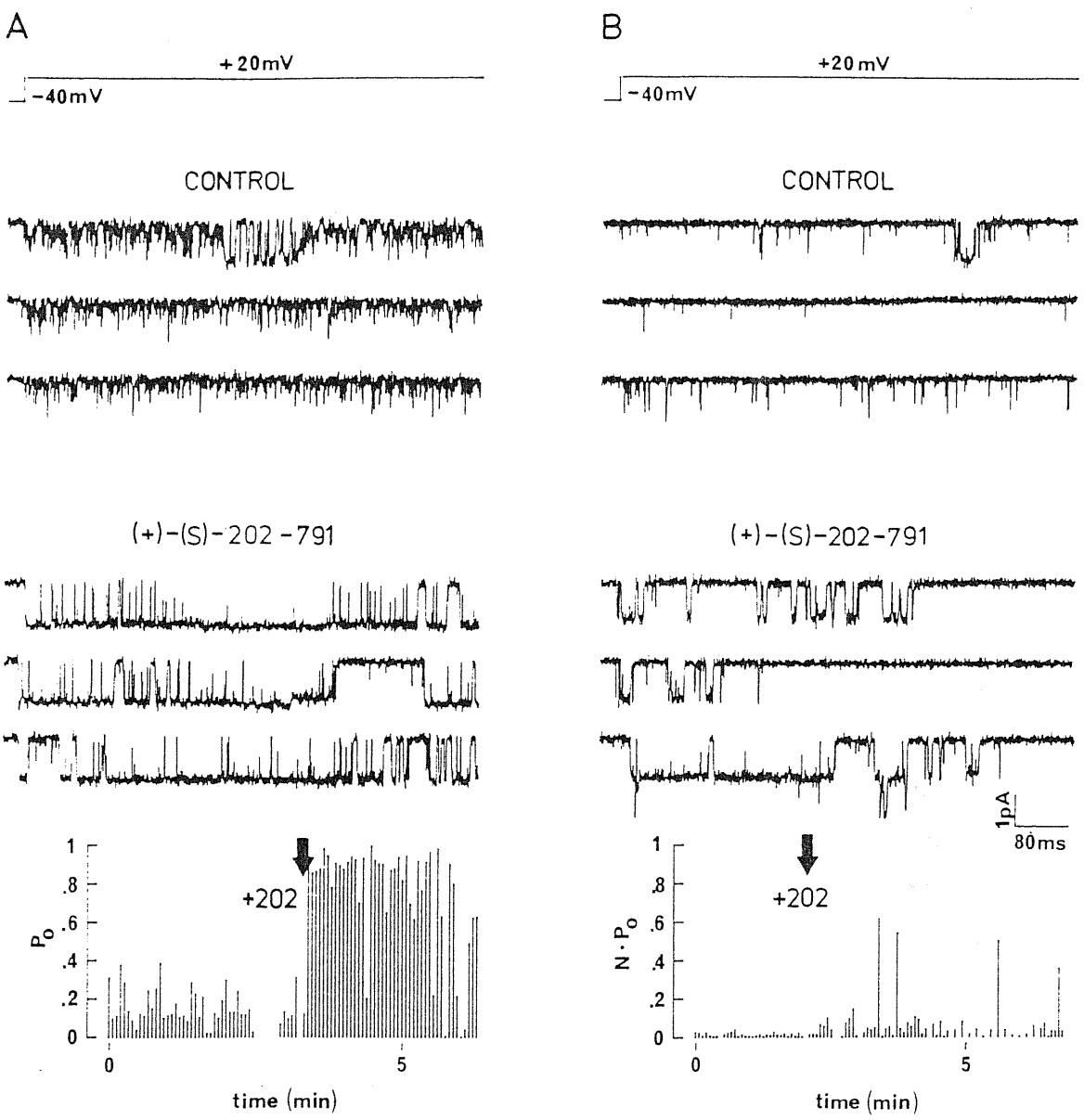

Figure 1. Two different DHP-sensitive cardiac-like gating patterns in cerebellar granule cells.

(A) Cell-attached recordings with 90 mM Ba^{2+} as charge carrier from a patch containing a single L-type Ca^{2+} channel and corresponding plot of open probability, p_o, versus time. Three representative current traces are shown before and after addition of (+)-(S)-202-791 (1 μM) to the bath. Bars in the p_o vs time plot represent the probability of channel openness at +20 mV in successive depolarizations. Depolarizations were 800 msec long and delivered every 4 seconds from holding potential= -40 mV. Records were sampled and filtered at 5 and 1 kHz, respectively. Cell N90G.

(B) Cell attached recordings from a patch containing 3 L-type Ca^{2+} channels and corresponding plot of Np_o (N=3) versus time. Voltage protocol and conditions as in (A). Cell N90F.

In many patches we observed a different single channel activity, characterized by sporadic short openings interrupted by rare longer openings and by a very low overall open probability, p_o (see control traces in Figure 1B). Upon addition of DHP agonist this type of activity changed into prolonged openings often grouped at the beginning of the depolarization and separated by long periods of silence (cf. the low Np_o in Figure 1B with N=3 channels in the patch). The two different DHP-sensitive gating patterns in Figure 1A and 1B have identical single channel conductance and currents. On the basis of our data we cannot distinguish whether they are different modes of activity of the same channel or, as it seems more likely, come from different L-type channel isoforms.

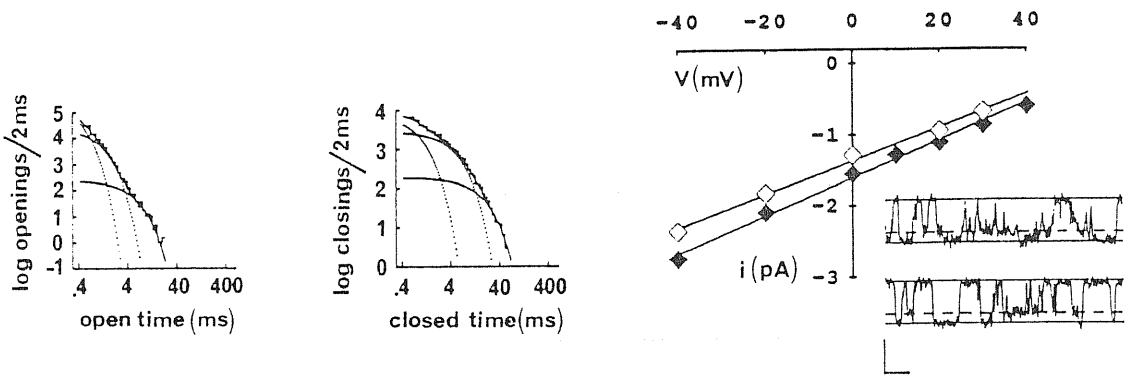

Figure 2. Properties of the cardiac-like DHP-sensitive gating pattern. (A) Log-log plots of the open and closed time distributions of a single L-type channel with gating similar to that in fig. 1A, in the absence of DHP agonist. V = +20 mV. The dark solid line in each plot is the best fitting sum of exponential components (minimum number of components indicated by the maximum likelihood test, see Experimental Procedures). Each exponential component is shown as a dotted line. Both distributions are best fitted by the sum of three exponential components with time constants of 0.2, 0.6 and 3.2 msec for the open times and 0.6, 3.5 and 13.8 msec for the closed times, and relative areas of 77, 22 and 1% for open times and 29, 57 and 14% for closed times. The fastest component for open times is poorly resolved. Cell N33D.

(B) Unitary current voltage relations for the main conductance level (closed symbols, g=27 pS) and the subconductance level (open symbols, g=24 pS) of L-type channels with gating similar to that in fig. 1A. The traces in the inset show transitions between the main conductance and the subconductance current levels at +20 mV, which were frequently observed during mode 2. Calibration bars: 10 msec, 1 pA. Cell N48B.

Figure 3 shows the single channel activity of cerebellar L-type Ca^{2+} channels displaying completely different and novel functional properties. Their activity in the absence of DHP agonist was typically very low, with sporadic fast unresolved openings and occasional short bursts of resolved openings with mean open time around 1 msec (Figure 3B). Upon addition of DHP agonist this sparse activity changed into a peculiar gating pattern with relatively short openings (mean open time around 2 msec at +20 mV, cf Figure 5A) and long closings. The average single channel conductance of cerebellar L-type channels with this distinctive gating pattern was 23 ± 0.49 pS (n=7, with i=1.34 ± 0.03 pA at 0 mV). Note that both elementary conductance and current values are close to those of the subconductance level of cerebellar L-type channels with cardiac-like gating shown in Figure 2.

We use the term "anomalous gating" to refer to the DHP-sensitive gating pattern in Figure 3, and the term "cardiac-like gating" to refer to both the DHP-sensitive gating pattern in Figure 1A and that in Figure 1B. An L-type channel with anomalous gating in a cell-attached patch showed the same type of gating after excision. The anomalous gating then does not arise from block by some intracellular factor. Out of 30 single channel patches, 15 contained an L-type channel with anomalous gating and 15 contained an L-type channel with cardiac-like gating. Out of 48 patches with two or three L-type channels, 8 contained L-type channels with anomalous gating, 13 contained L-type channels with cardiac-like gating, and the remaining 27 patches showed a mixture of the two gating patterns.

Usually a single L-type Ca^{2+} channel with either the anomalous or the cardiac-like gating at the beginning of the experiment showed the same type of gating until the end. However, in one out of the 30 single channel patches we observed a switch between gating patterns (Figure 4 and 5). The current traces in Figure 4A, recorded during consecutive depolarizations in the presence of DHP agonist, are representative of the single channel activity observed during the first 24 minutes of the experiment. The consecutive current traces in Figure 4B are representative of the activity observed after 24 minutes. Judging from the fact that overlapping openings were never recorded during the entire experiment the patch contained only one channel. The abrupt switching of the channel from the anomalous gating

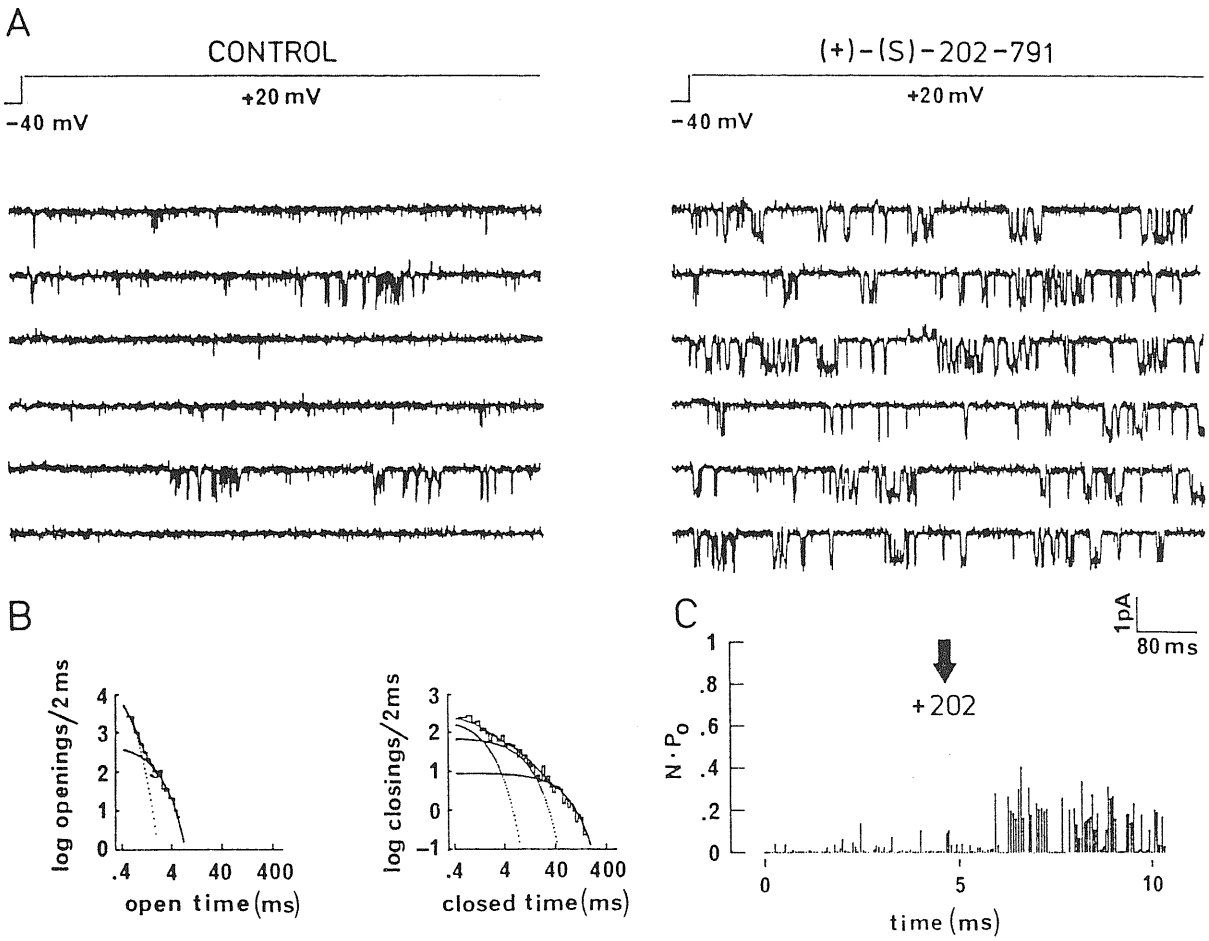

Figure 3. The "anomalous" DHP-sensitive gating pattern of cerebellar granules.
(A) Cell-attached recordings from a patch containing 2 L-type Ca^{2+} channels. Voltage protocol and conditions as in Figure 1. Six consecutive current traces are shown before and after addition of (+)-(S)-202-791 (1 μM) to the bath. Cell N83A. (B) Log-log plots of the open and closed time distributions of a single L-type channel with gating similar to that in (A), in the absence of DHP agonist. V = +20 mV. The open times are best fitted by the sum of two exponential components with time constants of 0.2 and 1.21 msec and relative areas of 93 and 7%, respectively. The fastest time constant is poorly resolved. The closed times are best fitted by three exponential components with time constants of 1.05, 6.93 and 45.9 msec and relative areas of 22, 44 and 35%, respectively. Cell N75B.
(C) Plot of Np_o (N=2) versus time for the experiment in (A). At the time indicated by the arrow, 1 μM (+)-(S)-202-791 was added to the bath. Cell N83A.

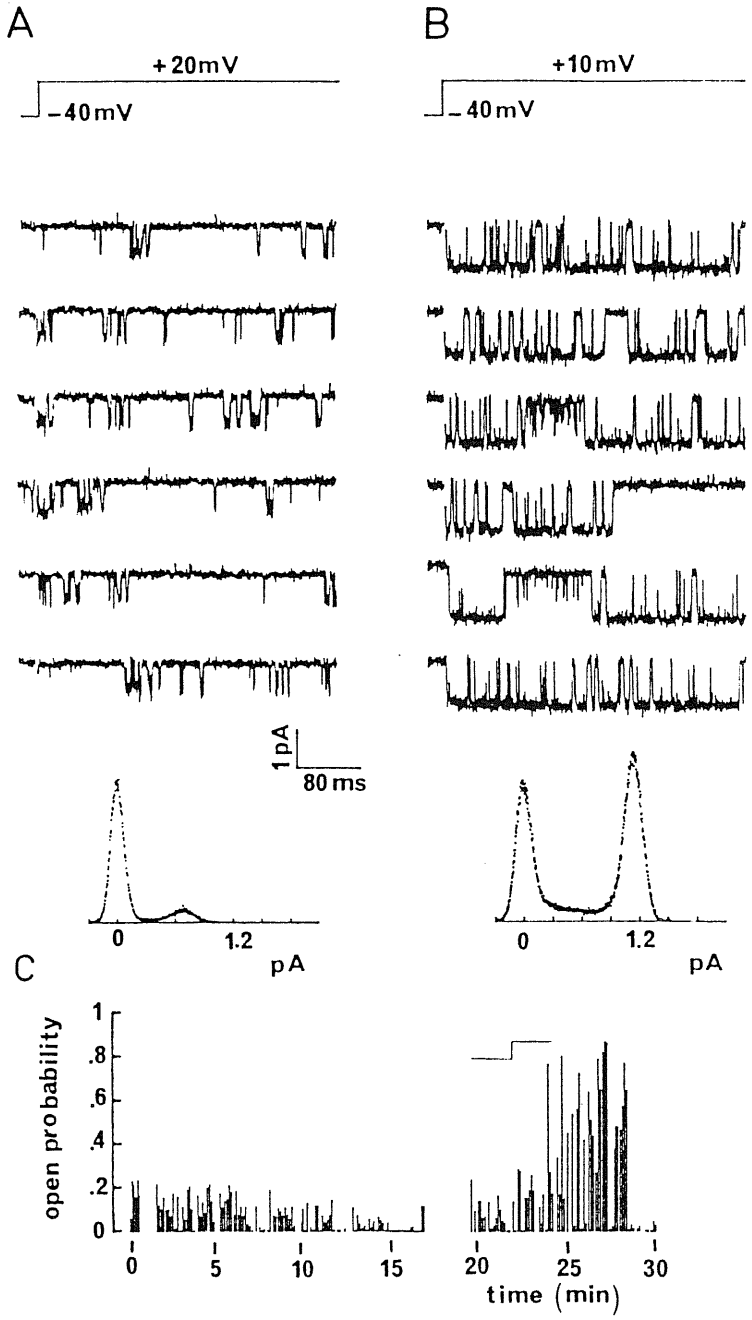

Figure 4. A single L-type Ca^{2+} channel switching from anomalous gating to cardiac-like gating. (A),(B) Cell-attached recordings from a patch containing a single L-type Ca^{2+} channel, in the presence of 1 μM (+)-(S)-202-791. (A) Consecutive current traces at +20 mV recorded during the first 24 minutes, and corresponding normalized current amplitude histogram. (B) Consecutive current traces at +10 mV recorded from the same patch after 24 minutes, and corresponding normalized current amplitude histogram. (C) Plot of p_o versus time. In the course of the experiment the test potential was changed from +20 mV to +10 mV at the time indicated by the small step in the plot. The sudden change in p_o, observed sometime later, reflects the switching between anomalous and cardiac-like gating patterns. Gaps along the time axis indicate periods in which the voltage protocol was changed, e.g. to obtain the i-V curve. Cell N57E in all panels.

to the cardiac-like gating is reflected by the sudden increase in single channel open probability during the experiment shown in Figure 4C. Figures 5A and 5B show histograms of the open and closed time durations for the anomalous and cardiac-like gating, respectively. In the anomalous gating the mean open time was more than five time shorter than in the cardiac-like gating, and the time constants of the three exponentials necessary to fit the closed time distributions were all larger than in the cardiac-like gating. As a result, as shown by the amplitude histograms under the

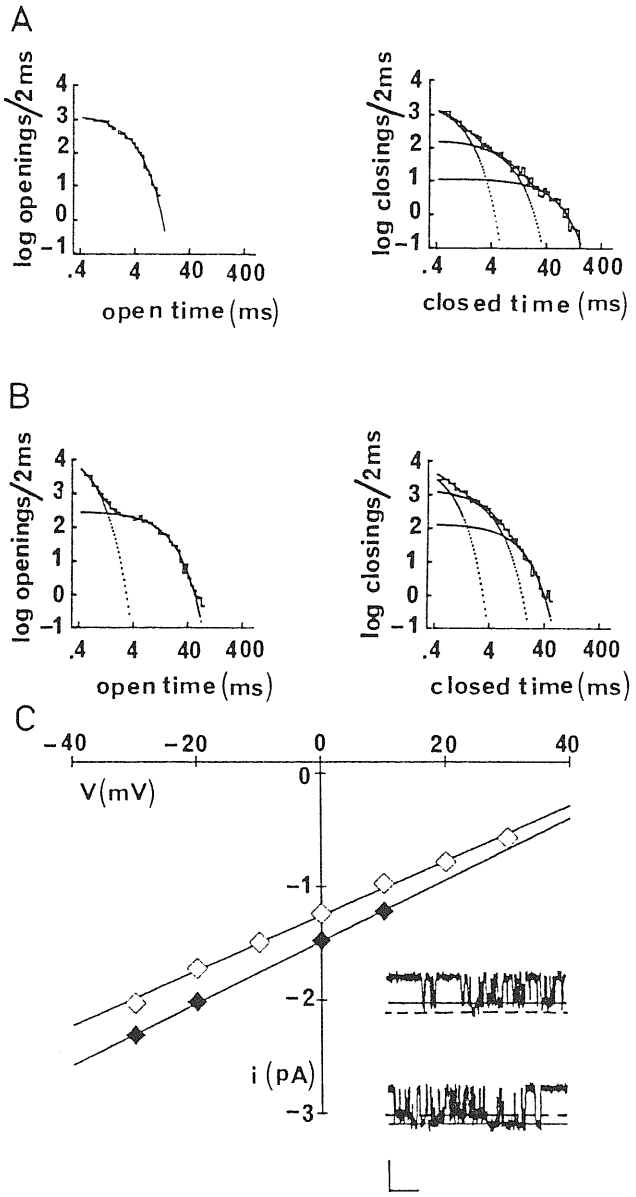

Figure 5. Open and closed time distributions and current-voltage relation for the anomalous and cardiac-like gating from a single channel patch.
(A),(B) Log-log plots of the open and closed time distributions for the gating patterns in fig. 4A (anomalous gating) and in fig. 4B (cardiac-like gating). (A) Anomalous gating. V = +20 mV. Open times are fitted by one exponential component with a time constant of 1.7 msec. Closed times are fitted by three exponential components with time constants of 0.59, 4.7 and 38 msec and relative areas of 55, 29 and 16 %, respectively. (B) Cardiac-like gating. V = +10 mV. Open times are fitted by two exponential components with time constants of 0.3 and 9.2 msec and relative areas of 68 and 32 %, respectively. Closed times are fitted by three exponential components with time constants of 0.4, 2.2 and 7.3 msec and relative areas of 42, 40 and 18 %, respectively. (C) Unitary current-voltage relations for the anomalous (open symbols, g = 24 pS) and cardiac-like (closed symbols, g = 27 pS) gatings. The top trace in the inset was selected to show a rare transition from the prevailing current level at +10 mV of the anomalous gating (solid line, i = .97 pA) to a short-lived higher current level (dotted line, i = 1.18 pA). The bottom trace shows rare transitions from the prevailing current level of the cardiac-like gating at +10 mV (i = 1.22) to a lower current level (i = .98). Calibration bar: 40 msec, 1 pA. Cell N57E in all panels.

traces, the open probability of the anomalous gating at +20 mV was much lower than that of the cardiac-like gating at +10 mV. This experiment confirmed that not only the gating properties but also the elementary currents and the single channel conductance were different between the two different gating patterns (Figure 5C). We observed within the cardiac-like gating rare transitions to a short-lived

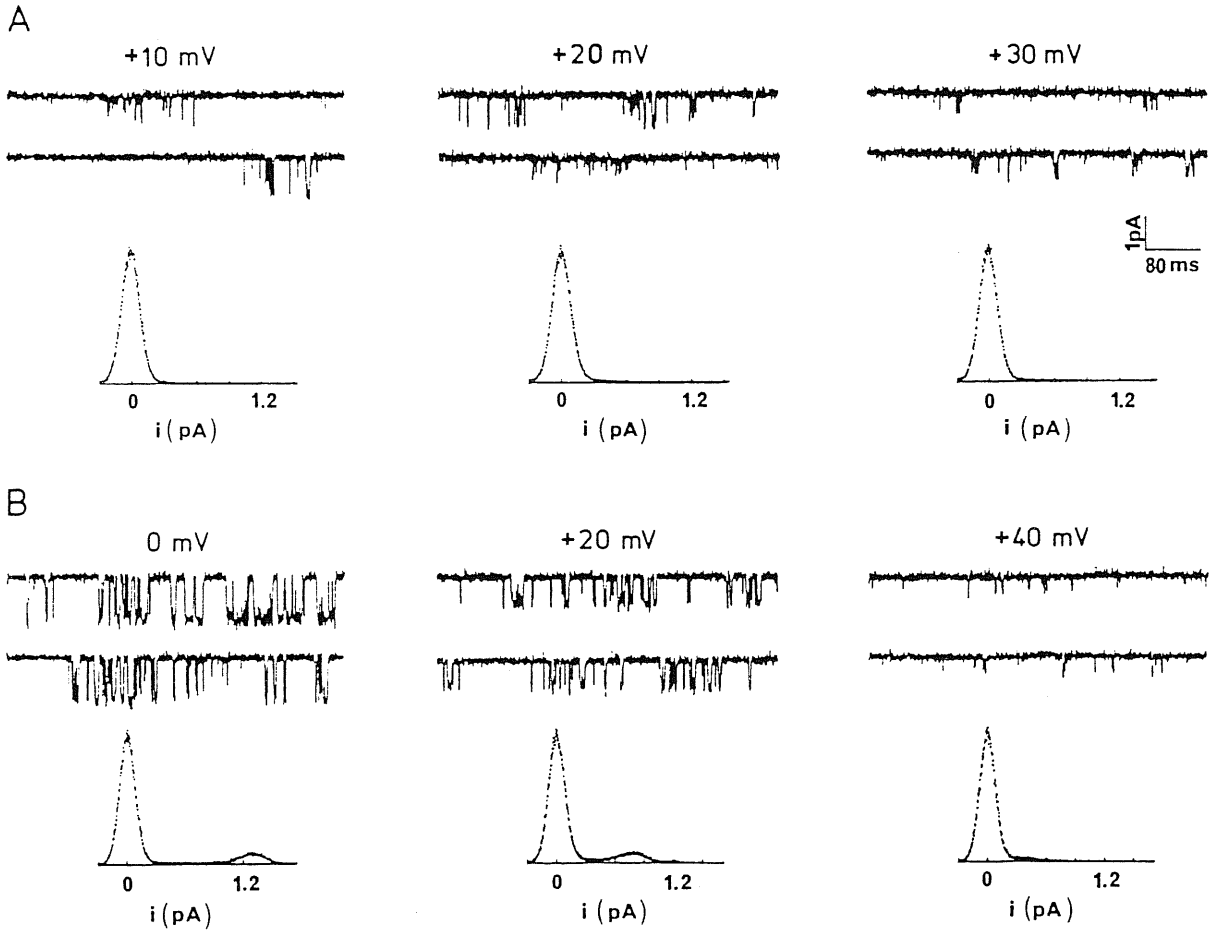

Figure 6. Voltage-dependent gating of L-type channels with anomalous gating.
(A) Cell-attached recordings from a patch containing a single Ca^{2+} channel. 800 msec long depolarizations to alternatively +10, +20 and +30 mV were delivered every 4 seconds from a holding potential of -40 mV. For each potential, two representative current traces and the normalized current amplitude histogram from all traces with activity are shown. Cell N75B
(B) Cell-attached recordings in the presence of 1 μM (+)-(S)-202-791 from a patch containing a single Ca^{2+} channel. Two representative current traces at 0, +20 and +40 mV and corresponding normalized current amplitude histograms. Depolarizations to the indicated voltages were alternated as in (A). Holding potential: -40 mV. Cell N74A.

subconductance state with unitary current similar to that of the anomalous gating. Even more rarely we observed within the anomalous gating brief transitions to a higher current level similar to that of the cardiac-like gating (see insets of Figure 5C).

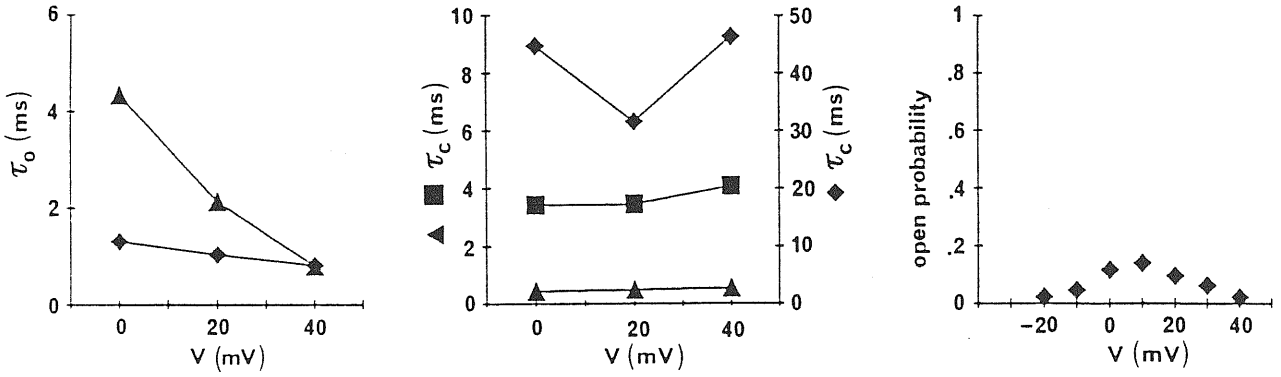

Fig. 7. Voltage dependence of open probability and open and closed times of L-type channels with anomalous gating.
(A) Voltage dependence of the time constants of the exponential components best fitting the open (τ_o) and closed (τ_c) time distributions for the experiment in (B). While two exponential components were required by the maximum likelihood test to fit the open times at 0 mV, one or two exponentials were equally likely at +20 and +40 mV. The plot contains the values of the biexponential fit. The relative area of the slow exponential component is 40% at 0 mV and 62% at +20 mV. The monoexponential fit at +20 mV gives τ = 1.8 msec. The best fit of the closed time distributions required a sum of three exponentials at each test potential. Cell N74A. (B) Voltage dependence of the probability of channel openness. 800msec long depolarizations were applied every 4 seconds to a cell attached patch containing two Ca^{2+} channels with anomalous gating, in the presence of 1 μM (+)-(S)-202-791. The different test potentials were alternated. Holding potential: -40 mV. p_o values are averages of the open probabilities measured in each sweep vith activity, at a given voltage. Cell N83A.

Unique properties of L-type channels with anomalous gating

While the voltage-dependent properties of cerebellar L-type Ca^{2+} channels with cardiac-like gating were similar to those reported for L-type channels in other cells, cerebellar L-type channels with anomalous gating showed unusual and remarkable voltage-dependent properties.

The amplitude histograms and the traces in Figure 6 show that both in the absence and in the presence of DHP agonist, when the test pulse voltage was increased, the open probability of L-type channels with anomalous gating remained very low.

Actually, Figure 7B shows that above +20 mV the open probability decreased instead of increasing. As shown in Figure 7A, this noticeable behaviour arised from both a shortening of the intervals of time spent in open states and a lenghtening of the intervals of time spent in closed states. In 3 different single channel experiments the open times decreased monotonically with voltage (overall range -20 to +40 mV) while the closed times varied non-monotonically with a minimum around +10/+20 mV.

Figure 8 shows a second noteworthy property of cerebellar L-type channels with anomalous gating. In the absence of DHP agonist, remarkably long openings separated by brief closings were often observed at -30 mV, after a depolarization to +30 mV during which channel activity was very low with sporadic short openings separated by long closings. In control traces at -30 mV without a previous depolarization openings were never observed (p_o=0). The average of the single channel traces at -30 mV following the depolarization gave a current that slowly decayed to zero with time constants of 13 and 126 msec. Figure 9 shows that the time course of the decay was voltage-dependent. The time constants of the biexponential fit of the average currents after a depolarization to +50mV increased roughly exponentially with voltage, with an e-fold change per 33.8 mV. At the beginning of the repolarization the average currents showed a hint of a rising phase, which originates from the fact that immediately after the depolarization the channels were often in a closed state before opening (cf. the representative traces in Figure 8). Long openings of DHP-sensitive Ca^{2+} channels at negative voltages with a certain delay after a depolarization have been previously reported in mouse cerebellar granule cells by Slesinger and Lansman (1991a). In our experiments, as in theirs, the probability of observing long openings at negative voltages increased with both the lenght and the magnitude of the predepolarization (not shown). However in contrast to their interpretation, we have several lines of evidences showing that these long openings are not reopenings during recovery from inactivation.

First of all, there were no signs of inactivation of single L-type channel activity during the preceding depolarization. This is shown by both the traces and the

Figure 8. Prepulse induced long openings at negative potentials of L-type channels with anomalous gating.
Cell-attached recordings from a patch with 2 L-type channels with anomalous gating, in the absence of DHP agonist. Selected current traces and average of 96 single channel current traces, obtained with the voltage protocol indicated above. Cell N26A.

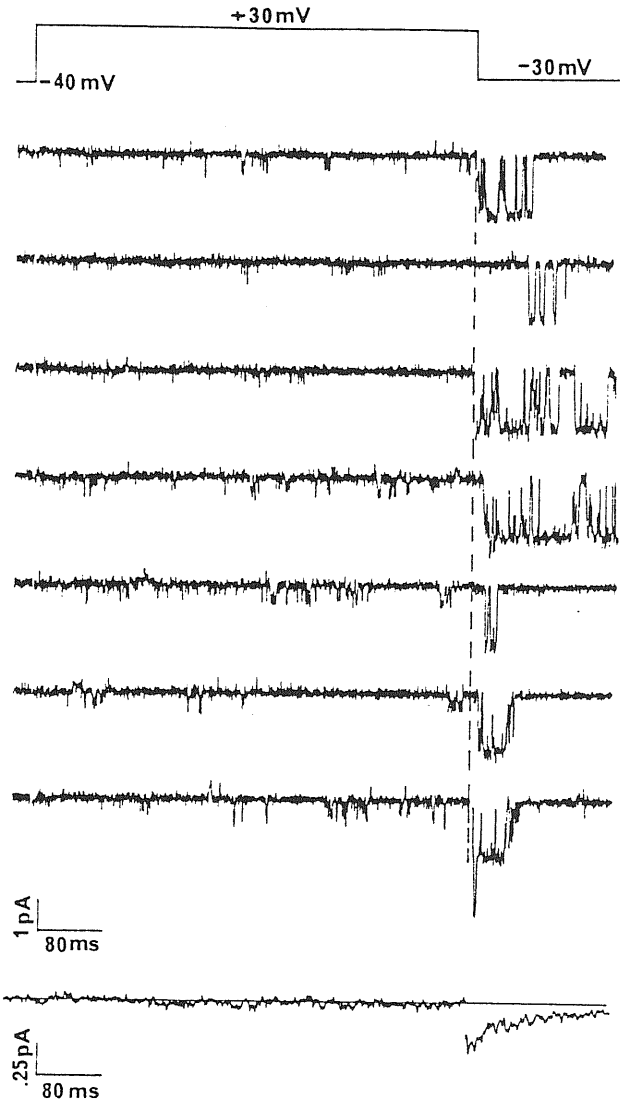

corresponding average current at +30 mV in Figure 8 in the absence of agonist, and perhaps even more clearly from the traces and the average current at +20 mV in Figure 10 from a similar experiment performed in the presence of DHP agonist. In this experiment there was only one channel in the patch. The voltage protocol of Figure 10 was alternated to control depolarizations to -20 mV.

Fig. 9. Voltage dependent decay of prepulse-induced currents.
Averaged single channel currents at different potentials, after a depolarization to +50 mV. Number of averaged records: n=36 at -10 mV, n=82 at -20 mV and n=167 at -50 mV. The patch contained at least 4 L-type channels. The decaying average currents were fitted by eye with the sum of two exponential components. The voltage dependence of the time constants of the biexponential fit is shown on the right. The solid lines are exponential fits (by eye) of the data points. Both time constants change e-fold per 33.8 mV. In some experiments, the decay of the prepulse-induced currents could be fitted by single exponentials, with time constants that changed e-fold per 33 mV. For comparison, the dotted line shows the voltage dependence of the time constant of the monoexponential decay of prepulse-induced average currents of cardiac L-type channels (from Pietrobon and Hess, 1990, shifted of 25 mV to take into account the different Ba^{2+} concentrations). In cardiac cells the decay has a more pronounced voltage dependence (e-fold change per 13.4 mV). Cell N25C.

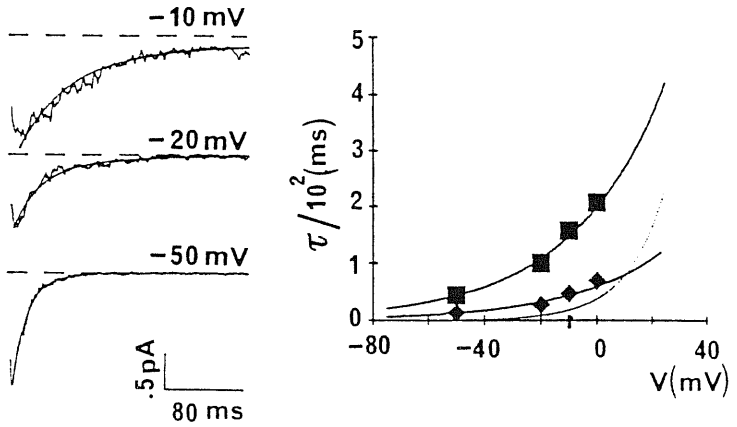

The representative traces in Figures 11 and 10 show that, while in some of the sweeps the activity of the channel at -20 mV after the depolarization to +20 mV was similar to that in the preceding control traces, in other sweeps the same channel showed a completely different activity, characterized by long lasting bursts of much longer openings. Episodes with similar long-lasting openings were observed very rarely in the control traces. As a result the average current at -20 mV after the predepolarization to +20 mV was potentiated with respect to the average current at -20 mV of the control traces (Figure 11).

Often immediately after the depolarization, the channel was closed before entering in the long-opening gating pattern. As a result, the average current after the depolarization disclosed a hint of a rising phase followed by a slow decay towards the value of the average control current. Figure 12 shows that the closed state

producing the rising phase was strictly linked to the long-opening gating pattern induced in some sweeps by the small predepolarization. In fact, using a discriminating value of $p_o = 0.4$ to separate the traces with the long opening gating pattern from those with activity similar to the control activity at -20 mV, the average current from the traces with $p_o \geq 0.4$ was greatly potentiated with respect to the average current of the preceding control sweeps and showed a very clear rising phase, while the average current from the traces with $p_o < 0.4$ was not significantly potentiated and displayed no sign of a rising phase. The open and closed time histograms in Figure 12 show that the long-opening gating pattern induced by the predepolarization ($p_o \geq 0.4$) had mean open times up to 5 times longer than those of the gating pattern prevailing in controls at -20 mV ($p_o < 0.4$).
The rising phase then does not reflect recovery from inactivation since i) the average current during the depolarization to +20 mV was constant, implying that the channel did not inactivate (Figures 8 and 10), and ii) after the depolarization the channel did not simply reopen but instead dwelled into a completely different set of open and closed states, which included the closed state accounting for the rising phase (Figure 10-12).

Voltage-dependent equilibrium between gating modes

Induction of a long-opening gating pattern of single L-type channels and potentiation of the Ca^{2+} current after positive prepulses have been previously observed in cardiac cells, and analysed in terms of a voltage-dependent equilibrium between gating modes (Pietrobon and Hess, 1990). The individual open and closed states of cardiac L-type channels giving rise to the short-opening gating pattern prevailing in control depolarizations, and those giving rise to the long-opening gating pattern induced by positive prepulses, were lumped into "modes" of gating. The two gating modes, here called mode 1 and mode 2 (as in Hess et al., 1984), were connected by single forward (k_f) and backward (k_b) first order rate constants (Figure 13A). k_f was found to increase and k_b to decrease with voltage (Pietrobon and Hess, 1990).

Figure 10. Prepulse induced long openings at negative potentials are not reopenings during recovery from inactivation.

Cell-attached recordings from a patch with a single Ca^{2+} channel with anomalous gating in the presence of 1 μM (+)-(S)-202-791. Control (800 msec long) depolarizations to -20 mV were alternated with the voltage protocol above the traces where the depolarization to -20 mV was preceded by a prepulse to +20 mV for 400 msec. The two protocols were separated by 4 seconds at -40 mV. Eight representative current traces showing unitary activity at -20 mV immediately after the prepulse and the activity at +20 mV during the prepulse, and corresponding averaged single channel currents (n=54). Cell N57E.

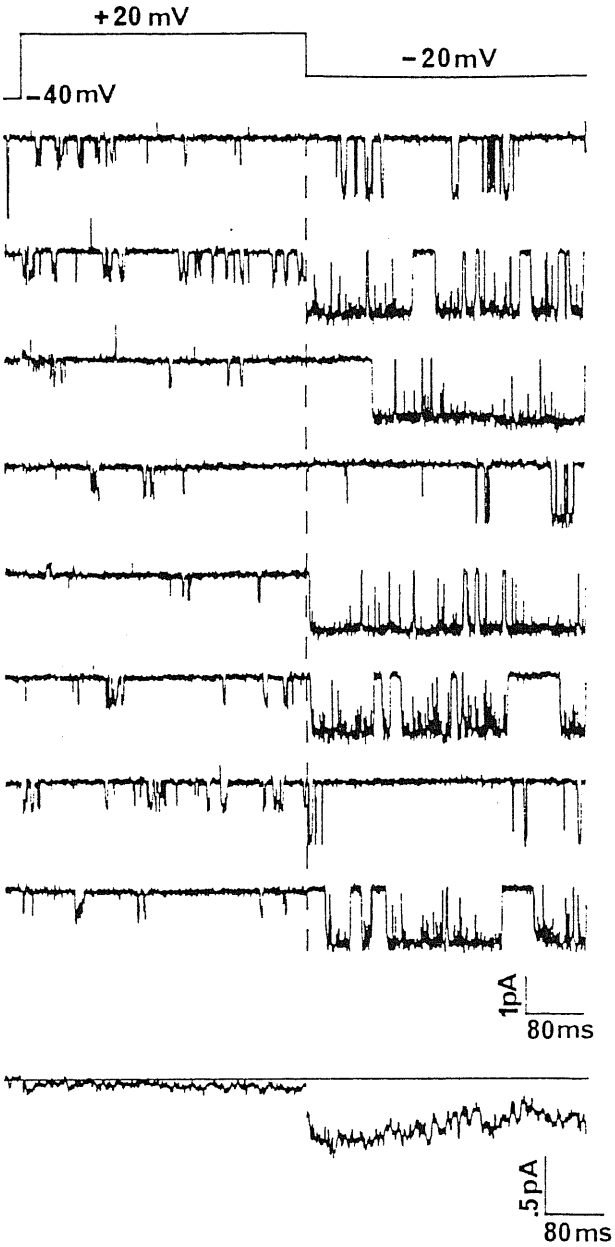

To explain, at least qualitatively, the peculiar properties of cerebellar L-type channels with anomalous gating, we considered a voltage-dependent equilibrium between gating modes analogous to that between modes 1 and 2 of cardiac channels, but with a crucial distinctive feature (figure 13B). In the set of states constituting each mode we connected the open state to an additional closed state, C_b in mode 1 and C_b^* in mode 2, and assumed voltage dependent rate constants for both entry

Fig. 11. Potentiation of the average current at negative potentials.
Cell-attached recordings from a patch with a single Ca^{2+} channel with anomalous gating in the presence of 1 μM (+)-(S)-202-791. Control (800 msec long) depolarizations to -20 mV were alternated with the voltage protocol above the traces where the depolarization to -20 mV was preceded by a prepulse to +20 mV for 400 msec. The two protocols were separated by 4 seconds at -40 mV (the same experiment as in fig. 10). Four couples of consecutive current traces showing unitary activity at -20 mV in controls and after the prepulse, and the corresponding averaged single channel currents (n=54). Cell N57E.

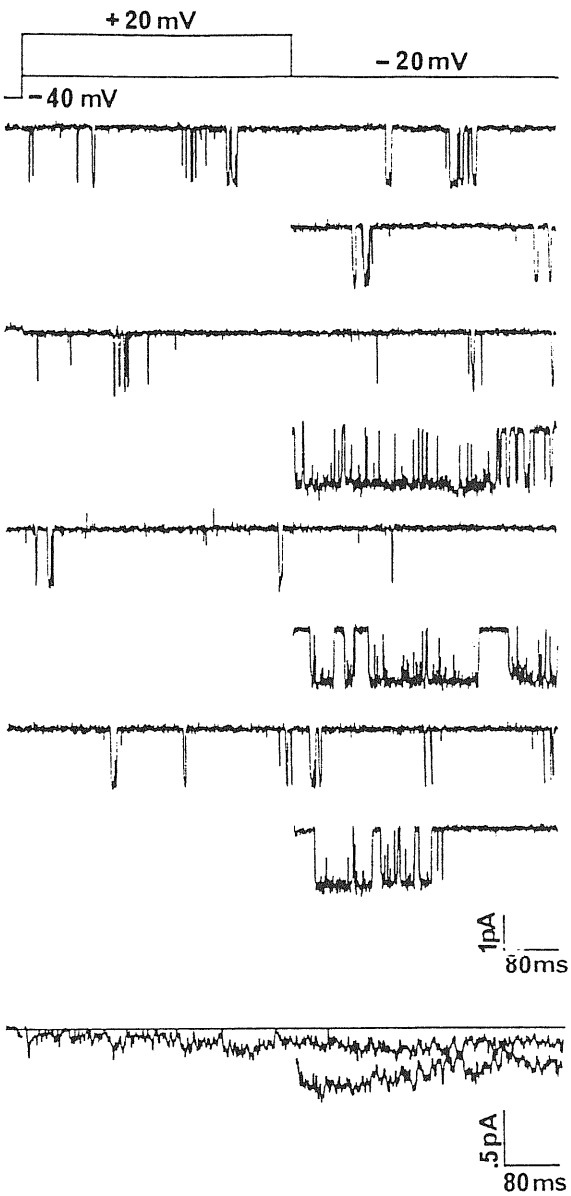

into (α, α^*) and exit from (β, β^*) C_b and C_b^*. α and α^* were assumed to increase and β and β^* to decrease with increasing voltage. All the peculiar gating properties illustrated in Figures 6-12 can be qualitatively explained by the kinetic scheme in Figure 13B, with values for the rate constants αs and βs such that the probability of finding the channel in the closed states C_b and C_b^* is practically zero at -20/-30 mV, but it becomes high at +20/+30 mV. We use the same scheme to discuss

results in the presence and absence of agonist because the two peculiar properties we are interested in discussing, i.e. the low open probability even at high positive voltages and the potentiation of the current at negative voltages following a predepolarization, were present with or without agonist with qualitatively similar features.

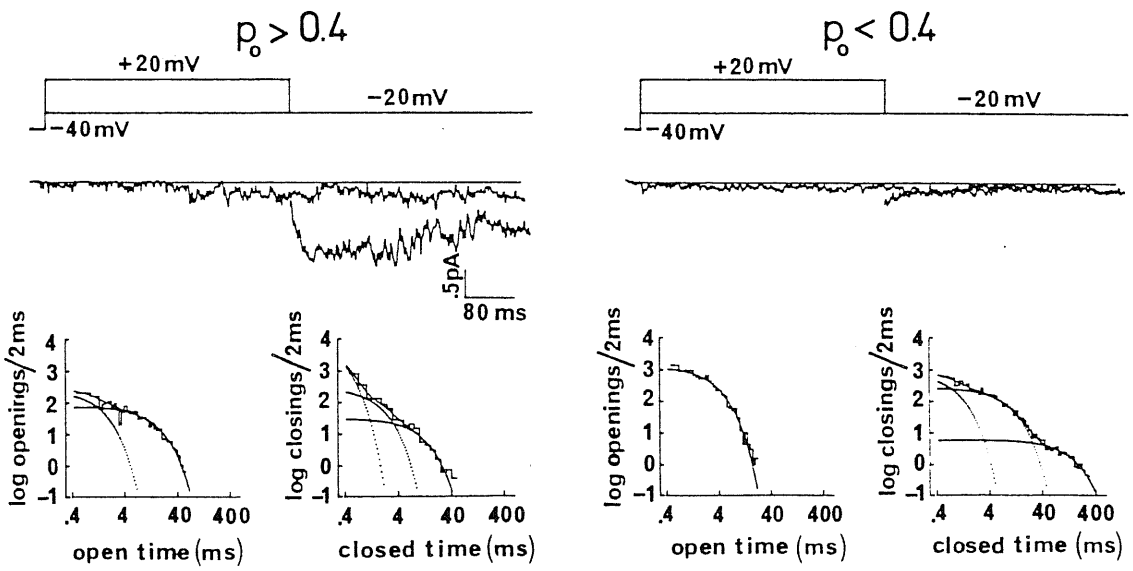

Fig. 12. The rising phase at negative potentials is linked with the induction of long openings.

Average single channel currents and log-log plots of open and closed time distributions from the experiment in fig. 10 and 11, after separation of the traces in two groups: those with the long-opening gating pattern at -20 mV after the prepulse ($p_o \geq 0.4$; n=16) and those with activity at -20 mV after the prepulse similar to controls ($p_o < 0.4$; n=38). Separation was achieved using a discriminating value of 0.4 for the open probability during 400 msec after the prepulse. The traces utilized for the averages of control currents were those immediately preceding the traces utilized for the averages of the currents after the prepulse. Open times at -20 mV of traces with $p_o \geq 0.4$ are best fitted by two exponential components with time constants of 0.9 and 11 msec and relative areas of 22.6 and 77.4%, respectively, while those of traces with $p_o < 0.4$ are fitted by a single exponential with $\tau = 2.4$ msec. Closed times are fitted by three exponential components with time constants of 0.2, 1.2 and 7.7 msec (relative areas: 73.4, 16.7 and 9.9%) for the traces with $p_o \geq 0.4$, and 0.6, 6.5 and 102 msec (relative areas: 11.5, 75.4 and 13.1%) for the traces with $p_o < 0.4$. Cell N57E.

The voltage dependence of the forward rate constant k_f connecting mode 1 and mode 2 explains the increased probability of observing the long-opening gating pattern at negative voltages after a predepolarization and the consequent potentiation of the average current (Figures 8,10,11 and 12). The voltage dependence of k_b, the backward rate constant from mode 2 to mode 1, explains the voltage-dependent decay of the potentiated current towards control values (Figure 9). The voltage dependence of the rate constants α^* and β^* within mode 2 explains the rising phase in the potentiated current immediately after a predepolarization. The rising phase reflects recovery from the closed state C_b^*, which is occupied by the channel for most of the time at positive voltages (where α^* is large and β^* is small), but becomes very unlikely at negative voltages (where α^* is small and β^* is large).

The voltage dependence of α^* explains also the fact that at positive voltages we never observed episodes of activity with long-lasting openings even during depolarizations that were effective in inducing the long-opening gating pattern at negative voltages (cf Figures 8-12). The long openings typical of mode 2 can be appreciated only at voltages where α^* is sufficiently small. With increasing voltages the mean open time of mode 2 shortens because α^* becomes larger. In Figure 7A in the presence of DHP agonist two exponential components were necessary to fit the open time histograms at voltages lower than 20 mV, where episodes of single channel activity with longer openings could be clearly distinguished from the prevailing activity (cf. first trace at 0 mV in Figure 6B). If we attribute the fast component to sojourns in the open state of mode 1 (O) and the slow component to sojourns in the open state of mode 2 (O^*), then a rapid increase of α^* with voltage can account for the rapid decline of the slow time constant (Figure 7A). At voltages > 10 mV usually the two time constants became similar. This similarity implies that at $V > 10$ mV mode 2 and mode 1 have similar mean open times, thus explaining why in Figure 6 the single channel activity at +20 mV during depolarizations that were effective in inducing mode 2 was indistinguishible from that during ineffective depolarizations. This analysis predicts that in the presence of DHP agonist, in contrast to the prepulse-induced potentiation of the current observed at negative

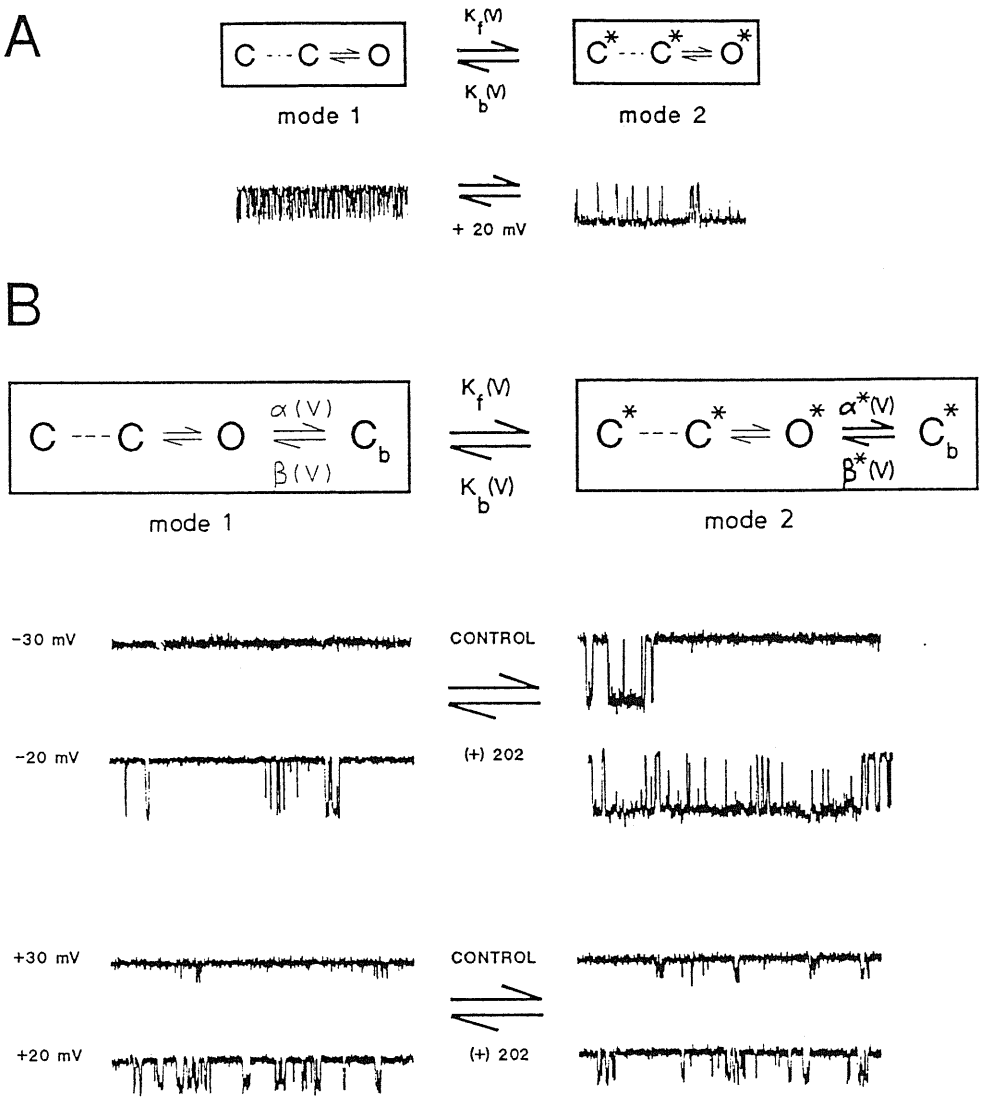

Figure 13. Simplified kinetic scheme with voltage-dependent equilibrium between gating modes.

(A) The kinetic scheme for cardiac L-type channels proposed by Pietrobon and Hess (1990). The two different set of states inside the boxes, which account for the short-opening and long-opening gating patterns in the underlying current traces at +20 mV, are lumped into "modes" of gating, here called mode 1 and mode 2. k_f and k_b, the rate constants of the transitions between mode 1 and mode 2, are voltage-dependent. See text.

(B) Simplified kinetic scheme modified from (A) to provide a qualitative explanation of the peculiar properties of cerebellar L-type channels with anomalous gating. In the two set of states inside the boxes an additional closed state is present, connected to the open state by voltage dependent rate constants. α and α^* are assumed to increase with voltage and to be small at -20/-30 mV and relatively large at +20/+30 mV. The opposite voltage dependency is assumed for β and β^*. See text. Below each set of states are the corresponding representative single channel current traces at negative (-20/-30 mV) and positive (+20/+30 mV) potentials, with and without DHP agonist.

voltages (cf Figure 11) there should be no prepulse-induced potentiation of the current at +20 mV. As predicted, in two experiments in the presence of DHP agonist, the unitary activity of L-type channels with anomalous gating at +20 mV after a prepulse to +50 mV was indistinguishible from that in control traces at the same voltage (not shown). In the absence of DHP agonist mode 1 and mode 2 at +20 mV can still be clearly distinguished, as shown from the traces and the biexponential open time histogram in Figure 3. The distinction becomes uncertain at +30 mV.

Finally, the voltage dependence of α, α^* and β, β^* explains the very low open probability typical of the anomalous gating, and the fact that p_o remains low and then starts to decrease with increasing voltages (Figures 6 and 7). Increasing voltages drive the channel from the open states to the closed states C_b and C_b^*, in addition to driving it, as usual, from the closed states in the activation pathway towards the open states. These opposing effects of voltage can explain the non monotonic voltage dependence of p_o (Figure 7B) and of some of the time constants of the closed time histograms (Figure 7A).

Most of the data of Slesinger and Lansman (1991a) can be explained at least qualitatively by the kinetic scheme in Figure 13B. However a clearcut interpretation of their findings is made difficult by the fact that most of their data are from multichannel patches held at -90 mV. At this holding potential, we have observed and characterized at least four different DHP-insensitive Ca^{2+} channels in rat cerebellar granule cells, one of which is particularly difficult to distinguish from L-type channels (Pietrobon et al., Soc. Neurosc. Abstracts, 1991; see Chapter 3). Almost certainly DHP-insensitive Ca^{2+} channels and L-type channels with both the cardiac-like and the anomalous gating coexist in the multichannel patches of Slesinger and Lansman (1991a,b).

Although we are aware that the kinetic scheme in Figure 13B is certainly an oversimplification and cannot quantitatively account for some of our own results (e.g. the biexponential decay of the potentiated current), we think it is useful as a conceptual framework for analysis of the complex behaviour of cerebellar L-type channels with anomalous gating.

Chapter 3

DHP-insensitive channels

All of the single channel activities that will be described in this chapter have been observed without apparent changes in channel gating in experiments done either in the absence or in the presence of the DHP agonist (+)-(S)-202-791 (1 μM) in the bath solution. They have thus been classified as DHP-insensitive channels.
Four different types of DHP-insensitive channels have been distinguished on the basis of differences in one or more of the following properties: single channel conductance, activation range, rate of inactivation, steady state inactivation range, gating kinetics (open and closed time distributions). The omega-conotoxin sensitivity of these channels has been tested.

C_1 channel

Fig. 1 shows the single channel activity of a first type of channel, named C_1, at three different voltages. Channel openings were fast events (approximately 0.5 msec mean open time, fig.2b), and thus non-fully-resolved openings events were frequently seen. The C_1 channel had an average single channel conductance (fig. 3) of 23.4 ± 0.60 pS (n=5; mean ± s.e.m.); the elementary current at 0 mV was 1.4 ± 0.04 pA (n=5;

mean ± s.e.m.).

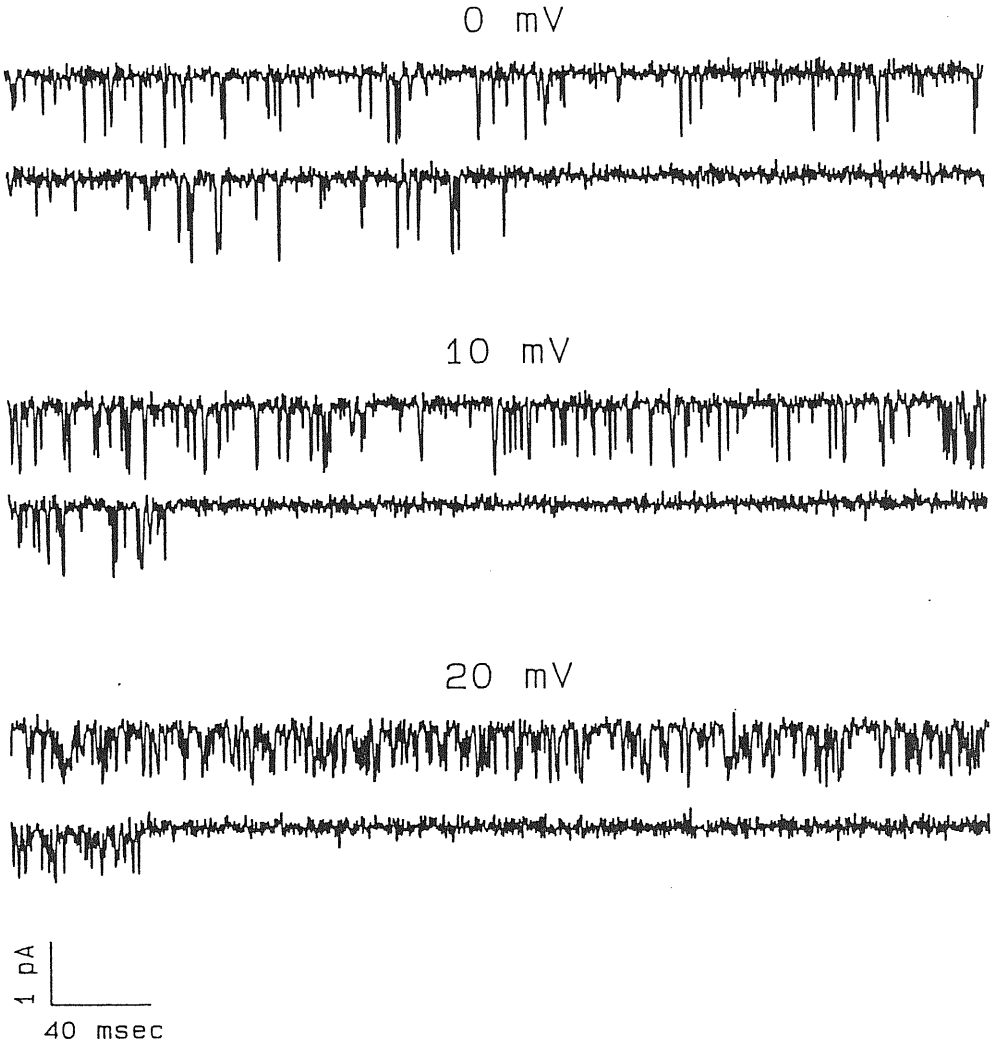

Fig.1. Cell attached recording from a patch containing one C_1 channel. Two selected records are shown for each set of depolarizations to 0, +10 and +20 mV from a holding potential of -80 mV. The first 400 msec of the response to depolarizations lasting 800 msec are shown. Depolarizations were delivered every 4 seconds. Ba_{2+} (90 mM) is the charge carrier, and the DHP agonist (+)-(S)-202-791 (1 μM) is present in the bath. Records were filtered and sampled at 1 and 5 Khz respectively. Cell N24E.

The channel started to activate at membrane potentials positive to -10 mV. The open probability increased with V, as can be seen from the average P_o versus V plot in fig. 2a, and also from the traces in fig. 1.

Upon prolonged depolarizations lasting 800 msec, in some records the C_1 channel

showed no inactivation, while in other records openings of the same channel were clustered at the beginning of the depolarization (fig. 4) (a similar switching between inactivating and non-inactivating activity has been previously described for N-type channels in sympathetic neurons (Plummer and Hess, 1991)).
This is reflected also in the mean current (fig. 4, bottom) averaged from many current traces in response to the same voltage protocol, where a decaying component as well as a maintained component are evident.

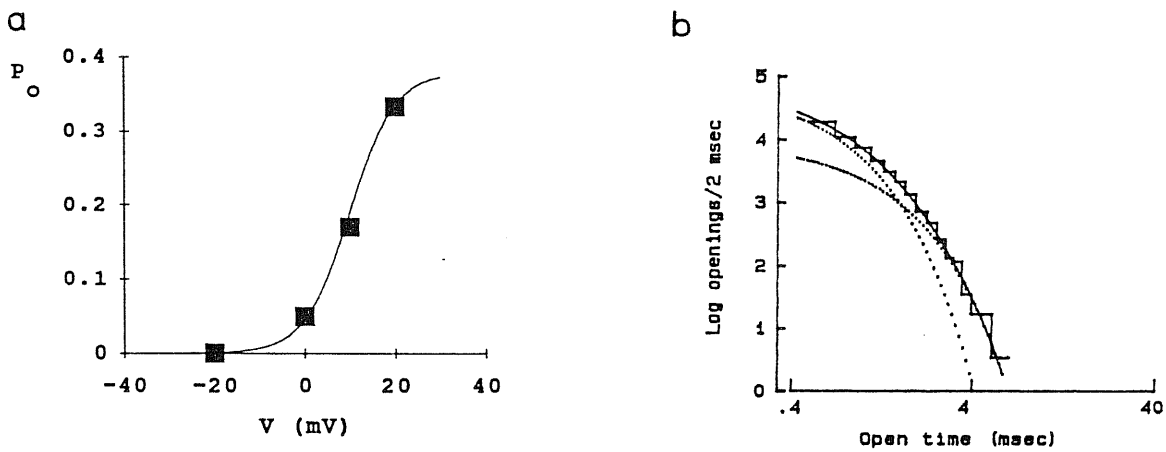

Fig. 2. Voltage dependence of open probability and open time distribution of a C_1 channel. (a) Plot of p_o versus test potential for a C_1 channel, from the same experiment as in fig. 1. p_o was measured as the steady-state open probability between the first and the last opening in a sweep. p_o at each potential is averaged over single p_o values computed from active traces. Traces with no openings (nulls) are not included. Solid line: fit to the relation $p_o = p_{o,max}/(1+\exp\{-z_eF(V-V_{1/2})/RT\})$ with values of $V_{1/2} = 10$ mV, $z_e = 5.14$ and $p_{o,max} = 0.38$.(b) Log-log plot (see Experimental Procedures) of the open time distribution for the same experiment. Test potential is +10 mV. The time constants of the best fit to data are around 0.5 msec.

The mean current should be equivalent to the macroscopic whole cell current generated by a population of C_1 channels during a single depolarizing pulse. The current decay should reflect transitions of a fraction of the C_1 channel population from a set of rapidly interconverting open and closed states to an inactivated state (or set of states).
C_1 also showed steady-state inactivation at relatively negative voltages: after

changing the holding potential from -100/-80 mV to -40 mV, in about one minute the activity in response to test depolarizations was lost. When the holding potential was returned to negative values, channel activity during positive voltage pulses was resumed (fig. 5).

Fig. 3. Elementary current-voltage relation of a C_1 channel
from the same experiment shown in fig.1. Conductance is 22 pS.

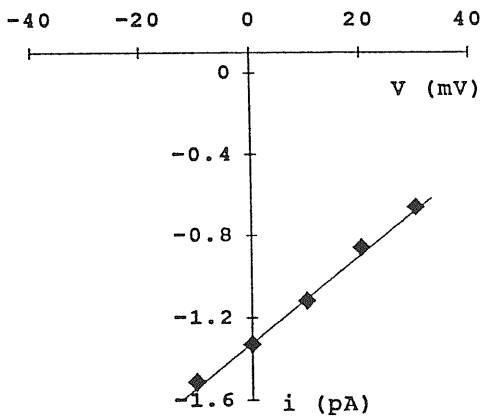

The effect of the N-type Ca^{2+} channel blocker omega-conotoxin GVIA on individual single channel activities has been rarely reported (see Ch. 1). This scarcity is justified by a technical difficulty. Omega-conotoxin acts on the Ca^{2+} channel from the external side of the plasma membrane (McCleskey et al., 1987). Thus,in a cell-attached experiment the toxin should reach its binding site from the solution inside the patch pipette. But the binding of omega-conotoxin to its receptor is competitively inhibited by the high concentration of divalent cations required to record from single HVA calcium channels (Cruz and Olivera, 1986; Mc Cleskey et al., 1987). A possible toxin inhibitory effect can not then be assessed by directly adding omega-conotoxin to the high Ba^{2+} solution inside the recording pipette because the probability of toxin binding in this condition is low. If a specific channel appears with toxin in the pipette, this would be of ambigous interpretation and would not imply insensitivity to the toxin.

To test the omega-conotoxin sensitivity of our channels, we used a strategy which takes advantage of the known irreversibility of omega-conotoxin block of N-type calcium current. If a toxin molecule previously bound to a receptor site in the patch

membrane remains bound for some minutes after establishing the contact between the cell membrane and the high-divalents-solution inside a patch-clamp recording pipette, then a statistical analysis of the fractions of cell-attached patches exhibiting activity in control conditions and after incubation with toxin should permit to assess sensitivity of a given channel to the toxin.

The evidence that this strategy was valid has been obtained with experiments on the neuroblastoma cell line IMR32.

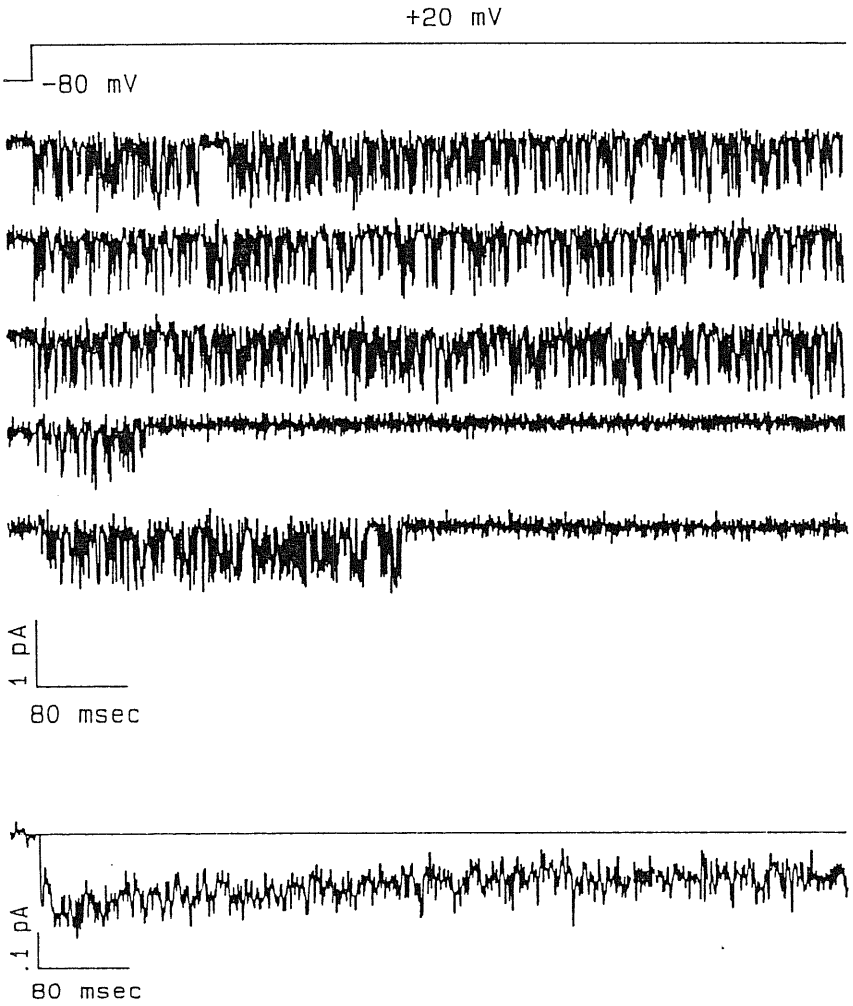

Fig. 4. Inactivation of the C_1 channel. Cell-attached recording from a patch containing 2 C_1 channels. **Top** 5 selected current records in response to 800-msec-long depolarizations following the voltage protocol indicated above the records. **Bottom** Mean current record obtained by averaging 50 similar current records, same experiment, same voltage protocol. Cell N02B

It has been reported (Carbone et al., 1990) that about 80% of the whole-cell calcium currents in these cells are inhibited after incubation for 30 minutes in 3.2 μM omega-conotoxin. This implies that a majority of the calcium channels in these cells should be omega-conotoxin-sensitive.

We thus performed a preliminary set of single channel recordings from cell-attached patches on IMR32 cells, and we identifyed a DHP-insensitive channel similar to the cerebellar C_1 channel in 75% of the patches (15 over 20 experiments; all experiments done in the presence of 1 μM +202 791 in the bath).

Next we tried to observe the omega-conotoxin effect by incubating the neuroblastoma cells in 3.2 μM omega-conotoxin in K^+-gluconate (0 Ca^{2+}) solution (see Experimental Procedures) for at least 30 minutes before performing patch-clamp experiments. In 20 experiments obtained in this conditions (1 μM +202 791 present in the bath) the C_1-like channel was never observed for at least 8 minutes after obtaining a seal.

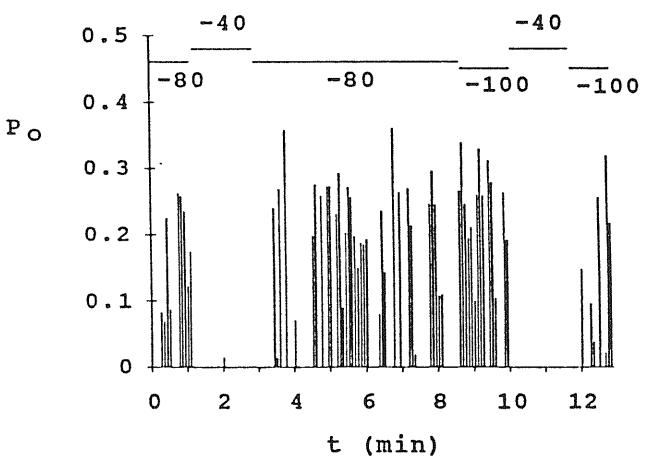

Fig.5. Steady state inactivation of the C_1 channel. (a) Plot of p_o versus time for the same experiment of fig. 4. Bars represent the open probability in successive 800-msec-long current traces in response to depolarization to +20 mV. The holding potential was changed as indicated above the graph.

From these experiments, a first conclusion is that the C_1-like channel is effectively an omega-conotoxin-inhibited calcium channel, as the statistics of channel rate of apparence with and without incubation with toxin are significantly different. As the gating properties of this channel are similar to those of our cerebellar C_1 channel,

this is a first indirect evidence supporting that the latter channel is an omega-conotoxin-sensitive channel. The main conclusion we inferred from these experiments is that omega-conotoxin-blocked channels remain blocked for some minutes even after coming in contact with a high concentration of divalent cations. We applied then the same experimental protocol used with IMR32 to the study of omega-conotoxin sensitivity of the C_1 channel of cerebellar granule cells. While the C_1 channel was found in more than 60% of the control experiments (10/16) where the appropriate voltage protocol was applied so as to allow the C_1 channel to open, in no one of 14 experiments done after incubation of the cells with the toxin the C_1 channel was seen. This result suggests that the C_1 channel is omega-conotoxin-sensitive.

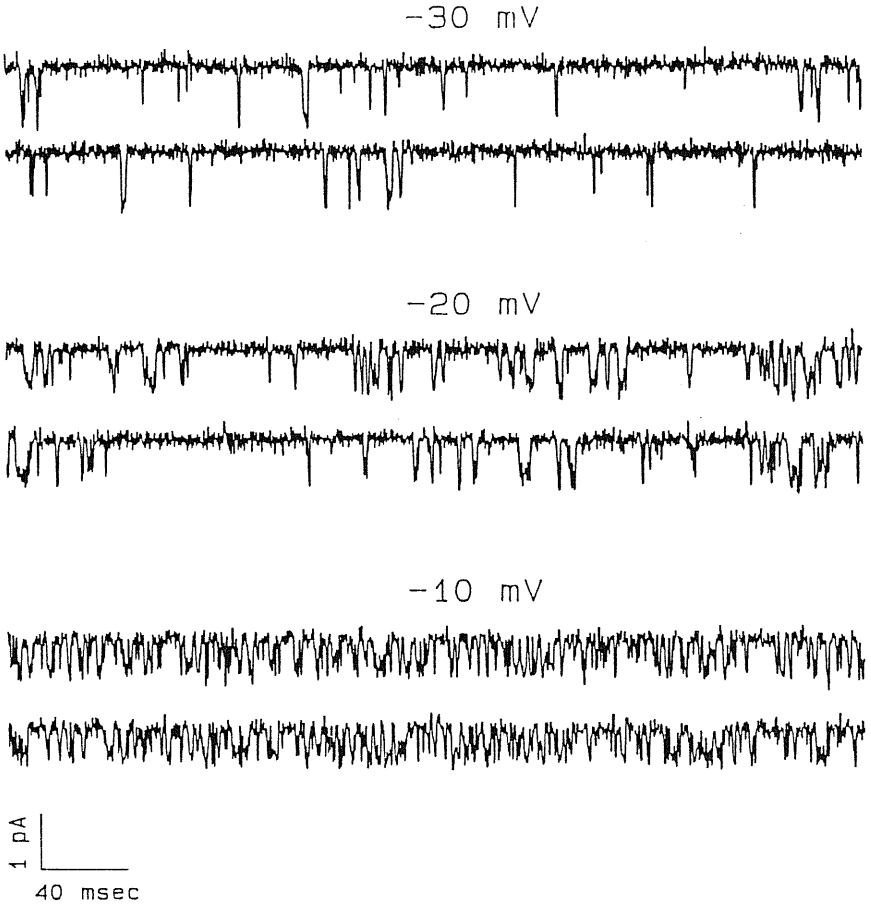

Fig. 6. Cell attached recording from a patch containing a C_2 channel. Two selected records are shown for each set of depolarizations to -30, -20 and -10 mV from a holding potential of -80 mV. The first 400 msec of the response to depolarizations lasting 800 msec are shown. Cell N02B.

C_2 channel

This second type of DHP-insensitive channel was found in cerebellar granules even more frequently than the C_1 channel.

The C_2 channel differed in various properties from the C_1 channel: it had smaller elementary currents and single channel conductance, a more negative activation range, different inactivation kinetics and longer mean channel open time (figures 6-10).

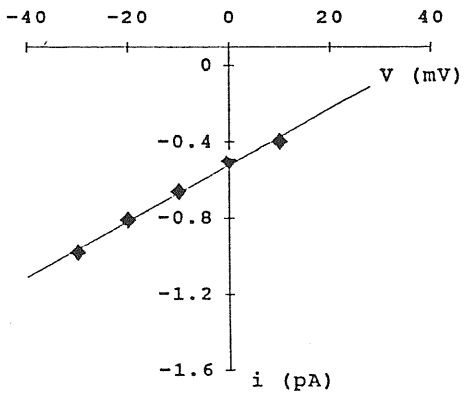

Fig. 7. Elementary current-voltage relation of a C_2 channel, from the same patch shown in fig. 6. Conductance is 15 pS.

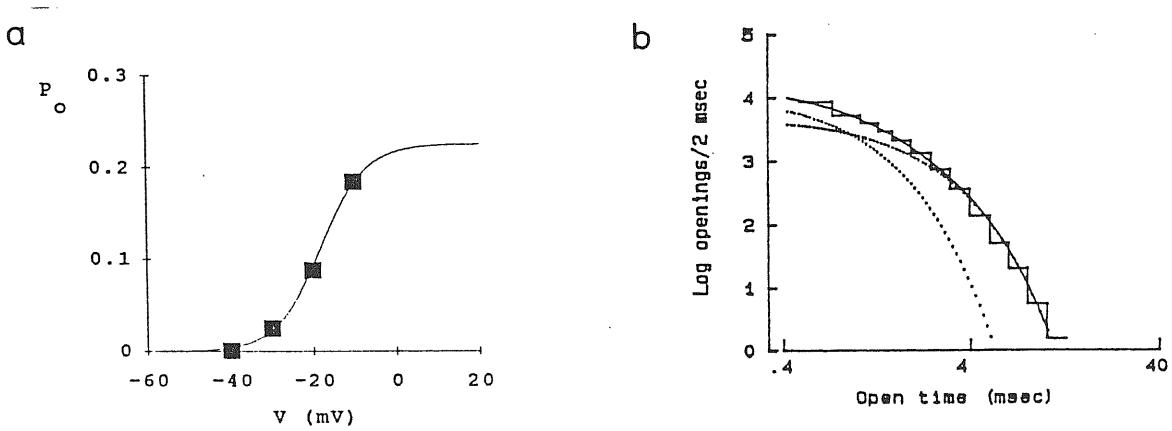

Fig. 8. Voltage dependence of open probability and open time distribution of a C_2 channel. (a) Plot of p_o versus test potential for a C_2 channel, from the same experiment of fig. 6. Solid line: fit to the relation $p_o = p_{o,max}/(1+\exp\{-z_e F(V-V_{1/2})/RT\})$ with $V_{1/2}$ = -18 mV, z_e = 4.67 and $p_{o,max}$ = 0.225. (b) Log-log plot (see Experimental Procedures) of the open time distribution for another patch containing a C_2 channel. Test potential is -20 mV. The time constants of the best fit to the histogram are 0.57 and 1.30 msec. Cell N03A.

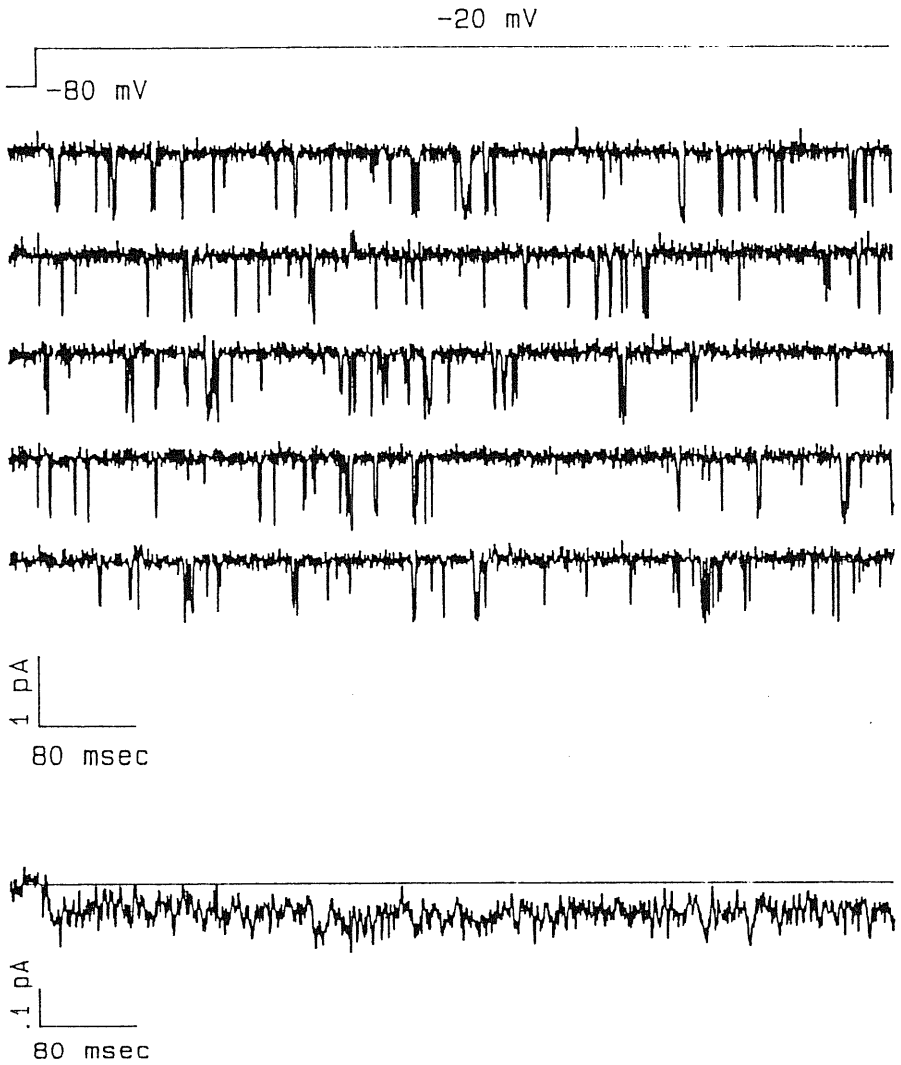

Fig. 9. Inactivation rate of the C_2 channel. Cell-attached recording from a patch containing three C_2 channel. **Top** 5 selected current traces in response to 800-msec-long depolarizations following the voltage protocol indicated above the records. **Bottom** Mean current averaged from 77 current traces from the same patch as in the upper part of the figure, same voltage protocol. Cell N03A

The typical activity of the C_2 channel at -30, -20 and -10 mV is shown in fig. 6. The mean duration of openings was slightly longer than for the C_1 channel, as is clear from comparison of fig. 6 with single openings of the C_1 channel (fig. 1, same time

scale), and as is confirmed by the fit to the respective open time distributions (fig. 2b and 8b). Some of the very fast openings in fig. 6 had a not fully resolved amplitude.The C_2 channel activated at membrane potentials positive to -40 mV, and its activity was clearly detected at -30 mV/-20 mV (fig. 6). The open probability increased in the range -30 to 0 mV (fig. 8a). At more positive potentials channel openings were not easily detected, due to the small current size. The elementary currents of the C_2 channel were smaller than those of C_1. Single channel conductance of the C_2 channel was 15.2 ± 0.54 pS (n=4; mean ± s.e.m.),and current amplitude was 0.5 ± 0.01 pA at 0 mV (n=4 ; mean ± s.e.m.; fig. 7). No sign of inactivation was detected even during depolarizing pulses lasting 800 msec (fig. 9). Correspondingly, the mean current obtained averaging over many traces did never show a decay with time (fig. 9, bottom). The holding potential highly influenced activity: the change from -80 mV/-100 mV to -40 mV produced a complete channel inactivation after about a minute, as one can appreciate in the experiment of fig. 10. The p_o in successive traces is reported versus time in fig. 10a, and the changes in holding potential are indicated by the legends above the plot.

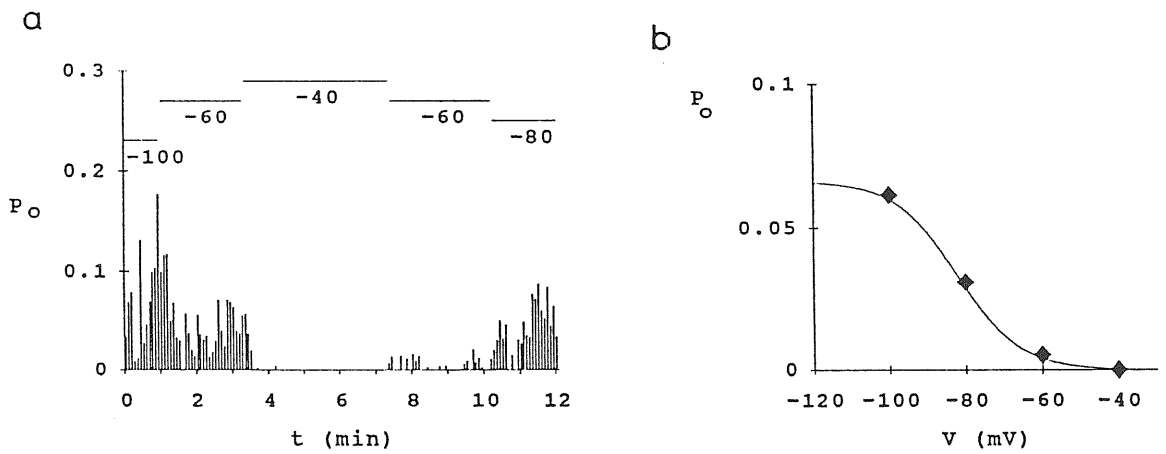

Fig. 10. Steady-state inactivation of the C_2 channel.(a) Plot of p_o versus time from the same experiment of fig. 9. p_o was computed for each successive 800-msec-long record during depolarization to -20 mV test potential. The holding potential was changed as indicated above the graph. (b) Plot of p_o at -20 mV test potential versus holding potential from the same patch. p_o at each potential is averaged over single p_o values from successive records, including records with no openings (nulls). Solid line: fit to the relation $p_o = p_{o,max}/(1+\exp\{z_eF(V-V_{1/2})/RT\})$ with $V_{1/2}$ = -83 mV, z_e = 3.21 and $p_{o,max}$ = 0.07.

In this particular experiment after repolarization of holding potential the activity resumed slowly, suggesting a very small rate of exit from inactivated states.

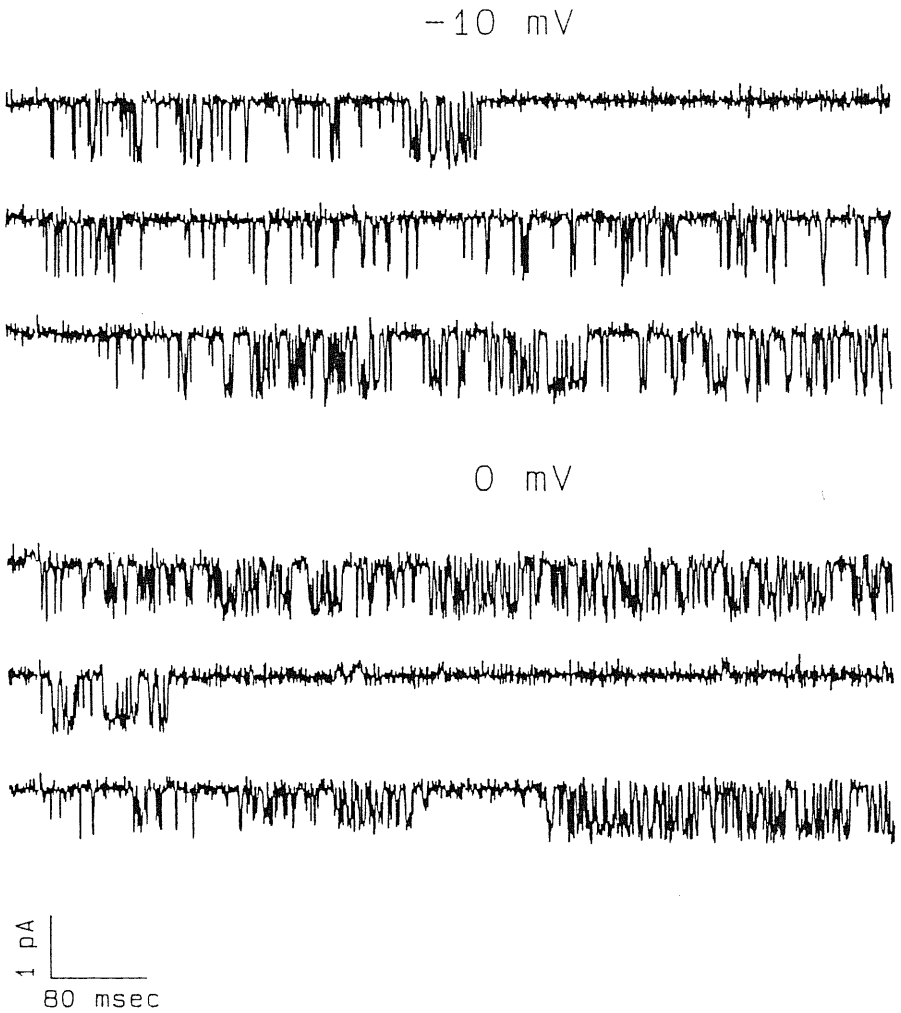

Fig. 11. Cell-attached recording from a patch containing two C_3 channels.
Three selected records are shown for each set of depolarizations to -10 and 0 mV from a holding potential of -80 mV. Cell N46C.

The sensitivity of the C_2 channel to omega-conotoxin GVIA was explored with the same strategy adopted for the C_1 channel (see above). In 6 over 8 experiments performed after incubating granule cells for >30 minutes in 3.2 μM omega-conotoxin, a C_2 channel was seen during the first 4 minutes of recording after

obtaining a seal. This should be enough to say that the C_2 channel activity is not inhibited by omega-conotoxin GVIA. The experiments to assess omega-conotoxin sensitivity were performed on neurons in culture from 7 to 11 days. We had previously observed a clear increase in the fraction of patches containing both C_1 and C_2 with increasing days in culture. Both channels were present in less than 5% of the patches on neurons from 1 to 3 days in culture and in more than 60% of the patches in neurons from 7 to 11 days in culture.

C_3 and C_4 channels

Although much less frequently (in <10% of the patches) than C_1 and C_2, other two DHP-insensitive channels were observed in cerebellar granules. A C_3 channel was observed which had intermediate properties between C_1 and C_2 in terms of conductance and activation and inactivation voltage ranges. Its typical activity is shown in fig. 11 for two different test potentials.

The elementary current was 0.8 ± 0.02 pA at 0 mV (n=3; mean ± s.e.m.) and the single channel conductance was 18.6 ± 0.54 pS (n=3; mean ± s.e.m.; fig. 12).

C_3 activated for voltages positive to -30 mV (fig. 13a), and steady-state inactivation was obtained after changing the holding potential from -80 mV to -40 mV (fig. 14; fig. 13b).

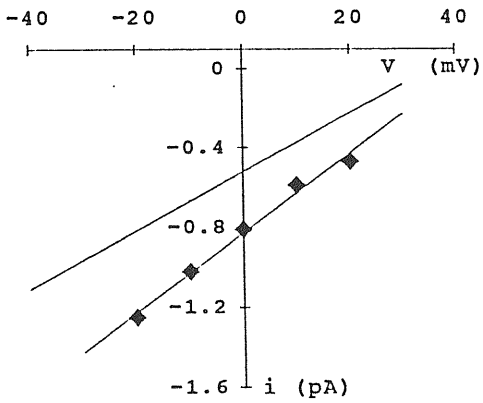

Fig. 12. Elementary current-voltage relation of a C_3 channel. In this experiment channel conductance is 20 pS. The best line through elementary current values for the C_2 channel is also reported for comparison. Cell N46C.

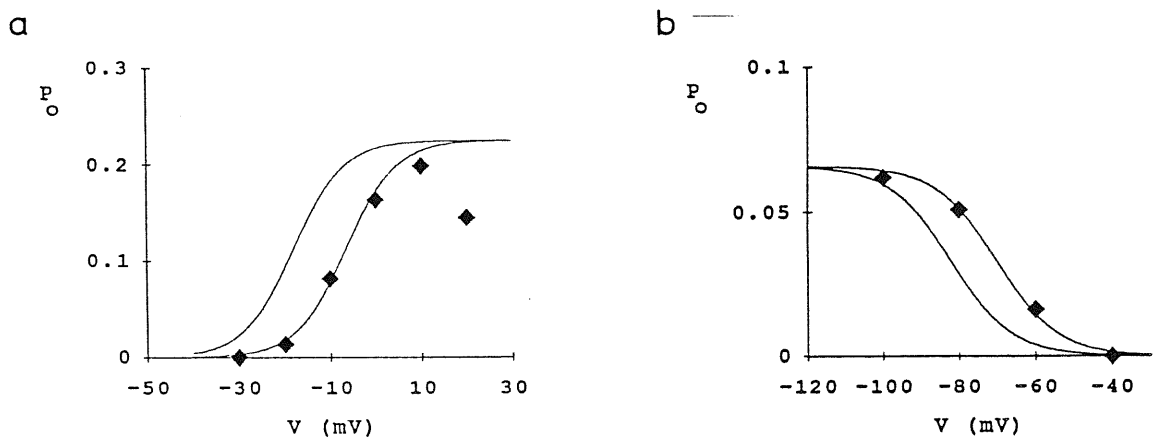

Fig. 13. Voltage-dependent activation and inactivation of the C_3 channel. (a) Plot of p_o versus test potential for the experiment of fig. 11. Solid line through symbols: fit to the relation $p_o = p_{o,max}/(1+\exp\{-z_eF(V-V_{1/2})/RT\})$ with $V_{1/2}$ = -6.5 mV, z_e = 4.67 and $p_{o,max}$ = 0.225. The second solid lines is reported for comparison with the curve fitting the same relation for the C_2 channel. (b) Plot of p_o versus holding potential from another patch with 2 C_3 channels. Test potential is -20 mV. Solid line through symbols: fit to the relation $p_o = p_{o,max}/(1+\exp\{z_eF(V-V_{1/2})/RT\})$ with $V_{1/2}$ = -71 mV, z_e = 3.21 and po,max = 0.07. Second solid line: fit of the same relation to the p_o versus holding potential plot for the C_2 channel. Cell N50D.

Fig. 14. Steady-state inactivation of the C_3 channel. Plot of p_o versus time for the same patch of fig. 11. p_o was computed for each successive 800-msec-long record during depolarization to +20 mV test potential. The holding potential was changed as indicated above the graph.

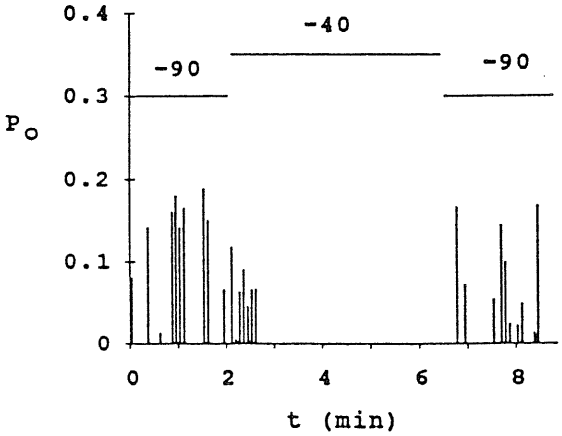

At variance from the C_2 channel, this channel did also show a small proportion of inactivating traces during depolarizations (fig. 11). The C_3 activity was clearly showed to be omega-conotoxin-insensitive. The activity of the last type of channel, named C_4, is shown in fig. 15 at five different test potentials. C_4 was similar to the

C_2 channel for several properties, namely single channel conductance (13 pS, fig. 16a), elementary current (0.5 pA at 0 mV), and activation threshold (activity started positive to -30 mV, fig. 16b); as the C_2 channel, it did not show a tendency to inactivation during 800 msec-long depolarizing test pulses (fig. 15).

But a remarkable difference from all the channels previously described is shown in fig. 17: the open probability of the C_4 channel did not change when the holding potential was varied in the range -90 to -20 mV. The C_4 channel was not sensitive to omega-conotoxin block.

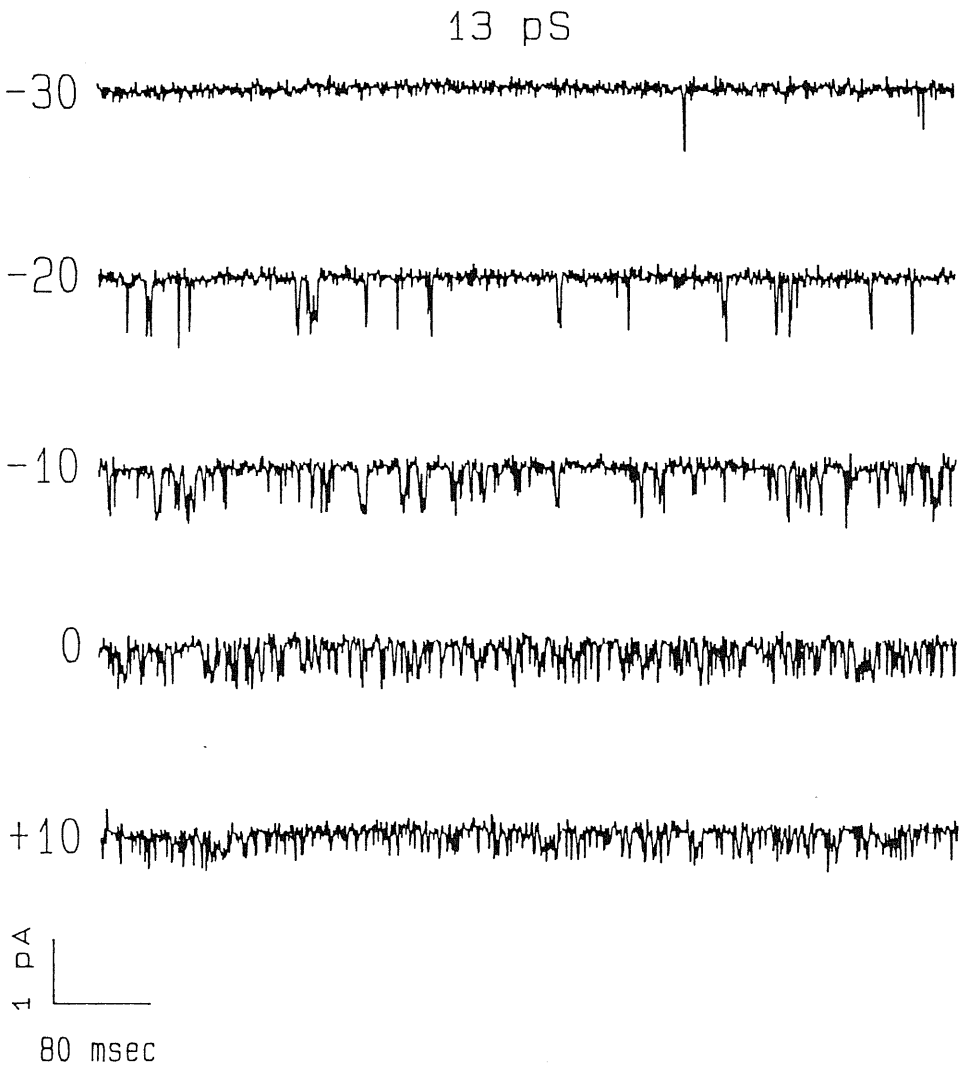

Fig. 15. Cell-attached recording from a patch containing one C_4 channel. One typical current record is shown for each of the five test potentials from -30 to +10 mV. Cell CE4A.

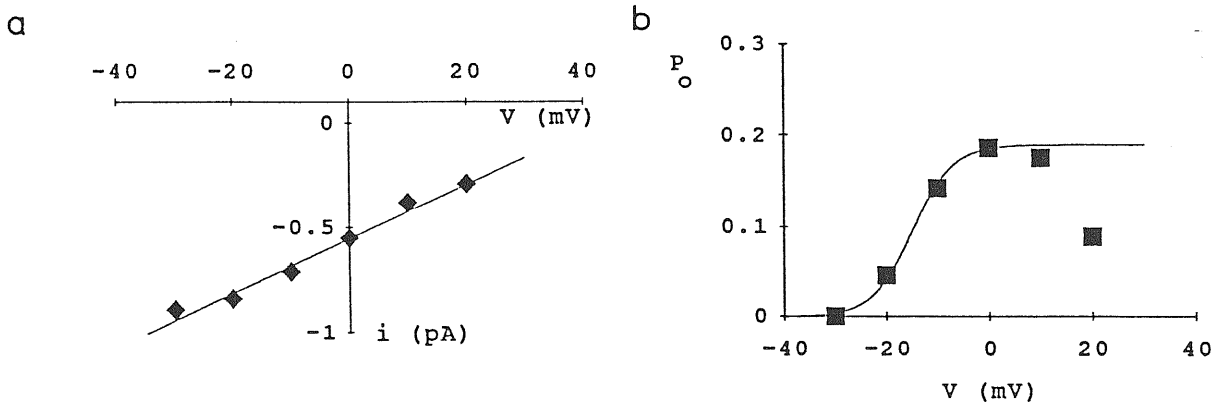

Fig. 16. Elementary current-voltage relation and open probability of the C_4 channel. Same patch as in fig. 15. (a) Single channel conductance is 13 pS. (b) Plot of p_o versus test potential for the same experiment.

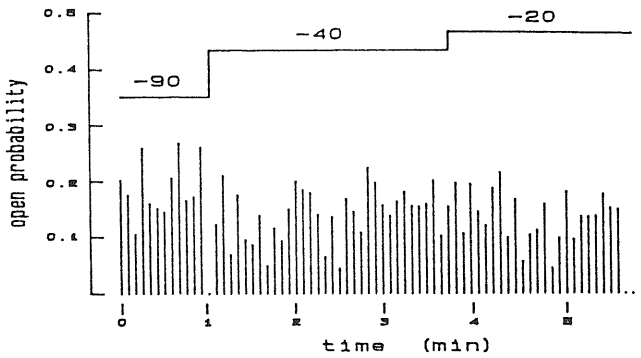

Fig. 17. The C_4 channel is unchanged by depolarized holding potentials. Plot of p_o versus time for an experiment with a C_4 channel. p_o was computed for each successive depolarization to 0 mV test potential. The holding potential was changed as indicated above the graph. Notice the absence of channel inactivation. Cell CE4A.

Chapter 4

Discussion

In the brain there are different α_1 subunits of DHP-sensitive (L-type) Ca^{2+} channels (Snutch et al., 1991; Williams et al., 1992). They are encoded by at least two different genes, and further diversity is created by alternative splicing of the two genes. Little is known about the functional consequences of the molecular diversity of brain L-type channels. Our results show that functionally different L-type Ca^{2+} channels coexist in rat cerebellar granule cells. We have observed two different DHP-sensitive gating patterns with single channel conductance and voltage-dependent properties similar to those reported for cardiac L-type channels, and a third DHP-sensitive gating pattern with novel and peculiar voltage-dependent properties, which we have called "anomalous gating". It is stimulating to hypothesize that the anomalous gating is generated by Ca^{2+} channels with a brain-specific subtype of DHP- sensitive (perhaps class D?) α_1 subunit different from the class C α_1 subunits that produce the cardiac-like gating patterns, and that the two cardiac-like gating patterns are produced by different isoforms of the class C α_1 subunits (Tsien et al., 1991; Williams et al., 1992). However, in the hypothesis that L-type channels with anomalous gating are different molecular entities from L-type channels with cardiac-like gating, the abrupt switch from the anomalous gating to the cardiac-like gating observed in one single channel patch becomes rather

puzzling. This experiment would rather suggest that the two gating patterns are different modes of activity of the same Ca^{2+} channel. However in this case, it appears difficult to explain the fact that we observed the two modes with about the same probability in different patches, but we observed a channel switching between the two modes only (once) in one patch.

Cerebellar L-type channels with anomalous gating have unusual voltage-dependent properties. On one hand, they open only rarely and briefly even at high positive voltages with open times that shorten with increasing voltage and closed times that decrease to a minimum and then increase with voltage. On the other hand, they show remarkably long openings at negative voltages after a positive prepulse, often with some delay after the depolarization. The probability of observing these prepulse-induced long openings increases with both the duration and the magnitude of the predepolarization. However they are not reopenings during recovery from inactivation (cf. Slesinger and Lansman, 1991a) since i) L-type channels with anomalous gating do not inactivate during predepolarizations effective in inducing long openings at negative voltages and ii) after the depolarization the Ca^{2+} channels do not simply reopen but instead enter into a different set of open and closed states.

The peculiar features of L-type channels with anomalous gating can be explained at least qualitatively in terms of a voltage-dependent equilibrium between gating modes, analogous to that between the short-opening mode (mode 1) and the long-opening mode (mode 2) of cardiac L-type channels (Pietrobon and Hess, 1990). Positive voltages shift the equilibrium towards mode 2 with consequent potentiation of the average current after a predepolarization. The peculiarity of the "anomalous gating" originates from the fact that here mode 2 is characterized by long openings with high open probability at negative potentials but by short openings with low open probability at positive potentials (see third section of Results and Figure 7). Thus, potentiation can be observed only at negative voltages. Even moderate depolarizations to +20/+30 mV (if sufficiently long) are capable to significantly shift the equilibrium of L-type channels with anomalous gating towards mode 2. Given the slow decay of the potentiated current, a progressive shift towards mode

2 would also be expected for trains of rapidly delivered short depolarizations. Presumably, Ca^{2+} influx through L-type channels with anomalous gating during a train of action potentials will critically depend on the frequency of the train, which sets the extent of progressive shift towards mode 2 and also the extent of Ca^{2+} influx in the interval between spikes.

A critical role of brain L-type channels in initiating Ca^{2+}-dependent intracellular regulatory events in postsynaptic cells in response to synaptic input has been proposed (Ahlijianian et al., 1990; Murphy et al., 1991; Johnston et al., 1992). The peculiar voltage-dependent properties of cerebellar L-type channels with anomalous gating make them very interesting transducers of electrical signals into chemical signals. In fact, they act as devices that give rise to little Ca^{2+} influx during a depolarization and to a large, potentiated Ca^{2+} influx upon repolarization after a long depolarization. L-type channels with anomalous gating appear then especially suited to generate a large surge of Ca^{2+} influx into postsynaptic cells following strong synaptic excitation, e.g. after a train of action potentials at high frequency. The timing of Ca^{2+} influx into the postsynaptic cell would depend on the lenght of the high-frequency train, while both lenght and strenght of synaptic excitation would establish the extent of Ca^{2+} influx. These properties make L-type Ca^{2+} channels with anomalous gating good candidates for mediating induction of certain forms of NMDA-receptor independent long term synaptic plasticity, for which an increase in postsynaptic intracellular Ca^{2+} has been shown to play a crucial role (Johnston et al., 1992). It will be interesting to establish whether L-type Ca^{2+} channels with anomalous gating are brain-specific and are present in other C.N.S neurons, in particular in hippocampal neurons, where long openings of L-type channels at negative voltages with some delay after a depolarization have been noticed (Fisher et al., 1990).

It has been recently reported that positive voltages promote phosphorylation of L-type channels in chromaffin cells (Artalejo et al., 1992). The voltage-dependent phosphorylation produce a change in gating pattern of the Ca^{2+} channels from one characterized by short openings with very low p_o to one characterized by long openings with very high p_o, with consequent potentiation of the Ca^{2+} current

(Artalejo et al., 1990; 1992). Although L-type channels with anomalous gating in cerebellar neurons and L-type channels in chromaffin cells have in common the extremely low open probability in control depolarizations, the voltage-induced potentiation of the Ca^{2+} current in cerebellar granules has kinetic properties totally different from that in chromaffin cells, and therefore is probably mediated by a different mechanism. Just to mention some of the main differences, in chromaffin cells the long-opening gating pattern and the potentiation after positive prepulses are not limited to negative test potentials, last much longer (up to 60 seconds) and are not observed in the presence of DHP agonist (Artalejo et al., 1990, 1991). It remains unknown whether positive membrane potentials shift the equilibrium between gating modes of cerebellar DHP-sensitive Ca^{2+} channels with anomalous gating through a mechanism intrinsic to the channel molecule or through some as yet unidentified cellular process (e.g modification of tonic interaction with a G protein, cf Kasai, 1991). Interestingly, it has been shown that the equilibrium between mode 1 and mode 2 of L-type channels is under humoral control both in cardiac and smooth muscle myocytes (Yue et al., 1990; Bonev and Isenberg, 1992).

Beside L-type Ca^{2+} channels, we have observed in cerebellar granule cells four types of DHP-insensitive channels, named C_1, C_2, C_3, and C_4. One of them, The C_1 channel, is an N-type channel, as revealed by its sensitivity to block by omega-conotoxin GVIA, while the other three channels are not. The C_1 channel has properties similar to a channel described in sympathetic neurons and in PC12 cells (Plummer et al., 1989, 1991); we have also frequently observed a very similar omega-conotoxin sensitive channel in single channel recordings on IMR32 cells. While the C_1 channel shows a mixed inactivating and noninactivating behaviour upon a prolonged depolarization, in contrast, the C_2, C_3, and C_4 channel do not inactivate during 800-msec long depolarizations. Steady-state inactivation develops at relatively negative potentials for the C_1, C_2, and C_3 channels, while the C_4 channel differs from them in not showing steady-state inactivation up to holding potentials of -20 mV.

Cerebellar granule cells then lend another evidence that sensitivity to holding potentiual can not be used as a criterion to separate L-type channels from other high-voltage activated calcium channels.

The DHP-insensitive channels in cerebellar granules have only slightly different single channel properties, and it would be hard to detect individual contributions to whole-cell currents. There is a gradual variation of activation ranges and elementary current between the C_4, C_3, C_2 and C_1 channels. But even slight variations of channel voltage-dependent properties might have a physiological relevance. Due to their relatively negative voltage range of activation, the C_2, C_3 and C_4 channels could participate in cell excitability processes, namely in the generation of calcium action potentials. However, the small difference in their activation threshold could give a different contribution to cell excitability. The C_1 channel, because of its relatively positive activation threshold, seems suited for producing a calcium influx in response to an action potential, and it could be involved in neurotransmitter release processes.

Cerebellar granule cells grown in primary cultures show evident electrical and morphological changes with days in vitro (Hockberger et al., 1987; Cull-Candy et al., 1989; Sciancalepore et al., 1989). Whole-cell calcium currents have been reported to increase in amplitude with days in vitro (Marchetti et al., 1991) and a DHP-insensitive calcium channel appearing from the 5th day in culture has been observed (Moran et al., 1992). In our experiments we also observed a clear increase in the frequency of appearance of the C_1 and C_2 DHP-insensitive channels with time in culture. It has been suggested that changes in culture might reflect stages of neuronal development occuring in vivo. Interestingly, N-type channels in cerebellar granule cells have recently been demonstrated to be specifically involved in the process of neuronal migration (Komuro and Rakic, 1992).

In conclusion, our single channel recordings on cerebellar granules show that functional diversity of calcium channels in neurons is wider than anticipated on the basis of pharmacology or macroscopic current measurements. Indeed, calcium channels in neurons might best be regarded as a family of channels with kinetic and

voltage-dependent properties that range along a continuum. The physiological significance of this large diversity probably lies in the possibility of fine tuning the entrance of the second messenger calcium, at the right place and the right time, through differential microscopic distribution and differential modulation of the different calcium channels subtypes.

Appendix

Experimental Procedures

Cell cultures

Cerebellar granule cells were grown in primary culture after enzymatical and mechanical dissociation from 8-day-old Wistar rats according to the procedure of Levi et al. (Levi et al. 1984).

The cells were plated on poly-L-lysine-coated glass coverslips and kept in Basal Eagle's medium supplemented with 10% fetal calf serum, 25 mM KCl, 2 mM glutamine and 60 μg/ml gentamycin. Cytosine arabinoside (10 μM) was added to the culture 18 hours after plating to inhibit the proliferation of non-neuronal cells.

Granule cells were the majority of the cells in the cultures, and were morphologically identified by the oval or round cell body, small size and bipolar neurites. Experiments were performed on granule cells grown from 1 to 12 days *in vitro*.

Patch-clamp recordings and data analysis

Single channel patch-clamp recordings followed standard techniques (Hamill et al., 1981). All recordings were obtained in the cell-attached configuration. Single channel currents were recorded with a DAGAN 3900 integrating patch-clamp amplifier, low-pass filtered at 1 Khz (-3 dB; 8-pole Bessel filter),
sampled at 5 Khz with a 12-bit INDEC (Sunnyvale, CA) AD/DA interface and stored for later analysis on a PDP-11/73 computer. The resolution of current measurements was to a precision of ≈ 1.5 fA (323.6 points/pA).
For the acquisition and the analysis of current records, computer programs written in BASIC-23 and running on the PDP-11/73 were used. Computer-programmed depolarizing voltage pulses were applied to the patch every 4 seconds; depolarizations lasted 800 msec.
In experiments aimed at the study of L-type channels, the holding potential was always -40 mV.

Linear leak and capacitative currents were digitally subtracted from all records used for analysis.
Open-channel current amplitudes were measured by manually fitting cursors to well-resolved channel openings and to the baseline current. In elementary current-voltage relations values at each voltage are averages of many measurements and standard errors are smaller than the symbol size.
A channel opening or closure was detected when >1 sampling point crossed a discriminator line setted at half of the elementary current (i) between open and closed level. Sampling points in the interval $[i\text{-}i/2, i+i/2]$ were considered sojourns to the open state, and points with value $<i/2$ were considered sojourns in the closed state. Histograms of open and closed time (lenght of sojourns to open or closed states) were fitted with sums of decaying exponentials. The best fit was determined by maximum likelihood maximization (Colquhoun and Sigworth, 1983) and the best minimum number of exponential components was determined by the maximum likelihood ratio test (Rao 1973; Horn and Lange 1983).

Log binning and fitting of the binned distributions was done as described by McManus et al. (1987) and Sigworth and Sine (1987). Notice that in log-log plots of fitted open- or closed-time distributions, the presence of an exponential component is signaled by a bump in the distribution of data. The dark solid line in each log-log plot is the best-fitting sum of decaying exponential components. Each exponential component is shown as a dotted line fitting the corresponding bump. Amplitude histograms were formed directly from the data, with bin width equal to the resolution of current measurement (323.6 points/pA). For display, each histogram was normalized to the value of the zero current peak, so that comparison of open probabilities from the relative areas under the non-zero current and zero-current peaks was easier.

In plots of open probability p_o versus test potential ('activation curve') the open probability in a record was computed as the ratio of the average current I in the record over the unitary single channel current, $p_o = \langle I \rangle / i$ (from recordings with only one channel; if more then one channel was present in the patch, p_o was computed from $p_o = \langle I \rangle / Ni$ with N = number of channels, by assuming the hypothesis of independent identical channels). The average was taken over the period between the beginning of depolarization and the end of the last opening in the record. Records with no openings (nulls) were not considered. Single p_o values from several records were then averaged to yield the value of p_o reported in the plot.

Plots of p_o versus holding potential ('inactivation curve') were instead obtained by computing $p_o = \langle I \rangle / Ni$ for the whole duration (800 msec) of each successive record in response to a depolarization, including null records. The test potential was kept constant, while the holding potential was varied, and individual p_o values obtained with the same holding potential were averaged and the average plotted versus V. This kind of measurement gives a parameter for describing the voltage-dependent transition to inactivated states.

A third kind of plot that was frequently used is the plot of p_o versus time. Here p_o was computed for each successive 800-msec-long record, and then reported as a bar

in the plot at the corresponding time along the experiment.

Pipettes and Solutions

Patch pipettes were pulled from Boralex hematocrit micropipettes (P5251; USA Scientific Plastics, Ocala, FL), coated with Sylgard (Dow Corning Corp., Midland, MI) and fire-polished. They had an average resistance, in standard solutions, of 2.5-4 MOhm.

The pipette solution contained either $BaCl_2$ 90 mM, TEACl 10 mM, CsCl 15 mM, Hepes 10 mM, (pH setted to 7.4 with TEAOH) or sometimes CsCl was absent and the TEACl concentration was changed to 30 mM. The bath solution was either K-Aspartate 140 mM, EGTA 5 mM, L-glucose 35 mM, Hepes 10 mM (pH setted to 7.4 with KOH), or K-Aspartate was substituted with the same concentration of K-gluconate. The high-potassium bath solution was used to zero the membrane potential outside the patch, so that the membrane potential was equal to minus the potential applied inside the recording pipette. To avoid block of calcium channels by contaminating heavy metal cations, great care was taken to avoid contact of all the solutions with metallic objects (e.g. syringe needles).

The DHP agonist (+)-(S)-202-791 (gift from Dr. Hof, Sandoz Co., Basle, Switzerland) was stored at 3 mM concentration in ethanol at -20°C. In experiments it was dissolved in the bath solution to the final concentration of 1 μM and added to the bath by gravity perfusion during experiments, or added to the bath before recording.

The toxin omega-conotoxin GVIA was dissolved in distilled H_2O at 166 μM and stored at -20°C. For use, the stock solution was dissolved in the bath solution (0 Ca^{2+}, K^+-Aspartate- or K^+-Gluconate-solution, see above) at the final concentration of 3.2 μM and neurons were kept in incubation in this solution for at least 30 minutes before recording.

Experiments were performed at room temperature (21-25°C).

References

Ahlijanian, M.K., Westenbroek, R.E., and Catterall, W.A. (1990). Subunit structure and localization of dihydropyridine-sensitive calcium channels in mammalian brain, spinal cord, and retina. Neuron 4, 819-832.

Aniksztejn, L., and Ben-Ari, Y. (1991). Novel form of long-term potentiation produced by a K^+ channel blocker in the hippocampus. Nature 349, 67-69.

Anderson, A.J., and Harvey, A.L. (1987). Omega-conotoxin does not block the verapamil-sensitive calcium channels at mouse motor nerve terminals. Neurosc. Lett. 82, 177-180.

Aosaki, T., and Kasai, H. (1989). Characterization of two kinds of high-voltage-activated Ca-channel currents in chick sensory neurons. Pflueg. Arch. 414, 150-156.

Artalejo, C.R., Ariano, M.A., Perlman, R.L., and Fox, A.P.(1990). Activation of facilitation calcium channels in chromaffin cells by D1 dopamine receptors through a cAMP-dependent mechanism. Nature 348, 239-242.

Artalejo, C.R., Mogul, D.J., Perlman, R.L., and Fox, A.P.(1991). Three types of bovine chromaffin cell Ca^{2+} channels: facilitation increases the opening probability of a 27 pS channel. J. Physiol., 444, 213-240.

Artalejo, C.R., Perlman, R.L., and Fox, A.P. (1992a). Omega-conotoxin GVIA blocks a Ca^{2+} current in bovine chromaffin cells that is not of the "classic" N type. Neuron 8, 85-95.

Artalejo, C.R., Rossie, S., Perlman, R.L., and Fox, A.P. (1992b). Voltage-dependent phosphorylation may recruit Ca^{2+} current facilitation in chromaffin cells. Nature 358, 63-66.

Bean, B.P. (1984). Proc. Natl. Acad. Sci. USA 81, 6388-6392.

Bean, B.P. (1989). Classes of calcium channels in vertebrate cells. Annu. Rev. Physiol. 51, 367-384.

Biel, M., Ruth, P., Bosse, E., Hullin, R., Stuhmer, W., Flockerzi, V., and Hofmann, F. (1990). Primary structure and functional expression of a high voltage activated calcium channel from rabbit lung. FEBS lett. 269, 409-412.

Bonev, A., and Isenberg, G. (1992). Arginine-vasopressin induces mode-2 gating in L-type Ca^{2+} channels (smooth muscle cells of the urinary bladder of the guinea pig). Pfluegers Arch. 420, 219-222.

Bossu, J.L., Dewaard, M., and Feltz, A. (1991a). Inactivation characteristics reveal two calcium currents in adult bovine chromaffin cells. J. Physiol. 437, 603-620.

Bossu, J.L., Dewaard, M., and Feltz, A. (1991b). Two types of calcium channels are expressed in adult bovine chromaffine cells. J. Physiol. 437, 621-634.

Campbell, K.P., Leung, A.T., and Sharp, A.H. (1988). The biochemistry and molecular biology of the dihydropyridine-sensitive calcium channel.Trends Neurosci. 11, 425-430.

Carbone, E., Sher, E., and Clementi, F. (1990). Ca currents in human neuroblastoma IMR32 cells: kinetics, permeability and pharmacology. Pfluegers Arch. 416, 170-179.

Catterall, W.A., Seagar, M.J., and Takahashi, M. (1988). Molecular properties of the dihydropyridine-sensitive calcium channel. J.Biol. Chem. 263, 3535-3538.

Cavalie', A., Pelzer, D., and Trautwein, W. (1986). Fast and slow gating behaviour of single calcium channels in cardiac cells: relation to activation and inactivation of calcium channel current. Pfluegers Arch. 406, 241-258.

Chin, H., Smith, M.A., Kim, H.L., and Kim, H. (1992). Expression of dihydropyridine-sensitive brain calcium channels in the rat central nervous system. FEBS Letters 299, 69-74.

Cohen, M.W., Jones, O.T., and Angelides, K.J. (1991). Distribution of Ca^{2+} channels on frog motor nerve terminals revealed by fluorescent omega-conotoxin. J. Neurosci. 11, 1032-1039.

Colquhoun, D., and Sigworth, F.J. (1983). Fitting and Statistical Analisys of Single-Channel Records. In Single Channel Recordings, B. Sakmann and E. Neher, eds. (Plenum, New York), pp. 191-264.

Cruz, L.J., and Olivera, B.M. (1986). Calcium channel antagonists. J. Biol. Chem. 261, 6230-6233.

Cuul-Candy, S.G., Marshall, C.G., and Ogden, D.C. (1989). Voltage-activated membrane currents in rat cerebellar granule neurones. J. Physiol. 414, 179-199.

De Jongh, K.S., Warner, C., and Catterall, W.A. (1990). Subunits of purified calcium channels α_2 and δ are encoded by the same gene. J. Biol. Chem. 265, 14738-14741.

Eckert, R., and Chad, J.E. (1984). Inactivation of Ca channels. Prog. Biophys. Mol. Biol. 44, 215-267.

Ellis, S.B., Williams, M.E., Ways, N.R., Brenner, R., Sharp, A.H., Leung, A.T., Campbell, K.P., McKenna, E., Koch, W.J., Hui, A., Schwartz, A., and Harpold, M.M. (1988). Sequence and expression of mRNAs encoding α_1 and α_2 subunits of a DHP-sensitive calcium channel. Science 241, 1661-1664.

Fakunding, J.L. and Catt, K.J. (1980). Dependence of aldosterone stimulation in adrenal glomerulosa cells on calcium uptake: effects of lanthanum and verapamil. Endocrinology 107, 1345-1353.

Fenwick, E.M., Marty, A., and Neher, E. (1982). Sodium and calcium currents in bovine chromaffine cells. J. Physiol. 331, 599-635.

Fisher, R.E., Gray, R., and Johnston, D. (1990). Properties and distribution of single voltage-gated calcium channels in adult hippocampal neurons. J. Neurophysiol. 64, 91-104.

Fortier, L.P., Trtemblay, J.P., Rafrafi, J., and Hawkes, R. (1991). A monoclonal antibody to conotoxin reveals the distribution of a subset of calcium channels in the rat cerebellar cortex. Mol. Brain Res. 9, 209-215.

Fox, A.P., Nowycky M.C., and Tsien, R.W. (1987a). Kinetic and pharmacological properties distinguishing three types of calcium currents in chick sensory neurones. J. Physiol. 394, 149-172.

Fox, A.P., Nowycky, M.C., and Tsien, R.W. (1987b). Single-channel recordings of three types of calcium channels in chick sensory neurones. J. Physiol. 394, 173-200.

Grover, L.M., and Teyler, T.J. (1990). Two components of long-term potentiation induced by different patterns of afferent activation. Nature 347, 477-479.

Hamill, O., Marty, A., Neher, E., Sakmann, B., and Sigworth, F.(1981). Improved patch-clamp techniques for high resolution current recording from cells and cell-free membrane patches. Pfluegers Arch. 391, 85-100.

Hess, P. (1990). Calcium channels in vertebrate cells. Annu. Rev. Neurosci. 13, 337-356.

Hess, P., Lansman, J.B., and Tsien, R.W. (1984). Different modes of calcium channel gating behaviour favoured by dihydropyridine Ca agonists and antagonists. Nature 311, 538-544.

Hess, P., Lansman, J.B., and Tsien, R.W. (1986). Calcium channel selectivity for divalent and monovalent cations. Voltage and concentration dependence of single channel current in ventricular heart. J. Gen. Physiol. 88, 293-319.

Hille, B. (1992). Calcium channels. In: Ionic channels of excitable membranes. Sinauer Associates Inc., Sunderland, Mass., pp. 83-114.

Hillmann, D., Chen, S., Aung, T.T., Cherskey, B., Sugimori, M., and Llinas, R.R. (1991). Localization of P-type calcium channels in the central nervous system. Proc. Natl. Acad. Sci. USA 88, 7076-7080.

Hirning, L.D., Fox, A.P., McCleskey, E.W., Olivera, B.M., Thayer, S.A., Miller, R.J., and Tsien, R.W. (1988). Dominant role of N-type Ca^{2+} channels in evoked release of norepinephrine from sympathetic neurons. Science 239, 57-61.

Hockberger, P.E., Tseng, H., and Connor, J.A. (1987). Immunocytochemical and electrophysiological differentiation of rat cerebellar granule cells in explant cultures. J. Neurosci. 7, 1370-1383.

Horn, R., and Lange, K. (1983). Estimating kinetic constants from single channel data. Biophys. J. 43, 207-223.

Hoshi, T., Rothlein, J., and Smith, S.J. (1984). Facilitation of Ca^{2+}-channel currents in bovine adrenal chromaffin cells. Proc. Natl. Acad. Sci. USA 81, 5871-5875.

Jay, S.D., Ellis, S.B., McCue, A.F., Williams, M.E., Vedvick, T.S., Harpold, M.M., and Campbell, K.P. (1990). Primary structure of the γ subunit of the DHP-sensitive calcium channel from skeletal muscle. Science 248, 490-492.

Jay, S.D., Sharp, A.H., Kahl, S.D., Vedvick, T.S., Harpold, M.M., and Campbell, K.P. (1991). Structural characterization of the dihydropyridine-sensitive calcium channel α_2-subunit and the associated δ peptides. J. Biol. Chem. 266, 3287-3293.

Johnston, D., Williams, S., Jaffe, D., and Gray, R. (1992). NMDA-receptor independent long-term potentiation. Annu. Rev. Physiol. 54, 489-505.

Jones, O.T., Kunze, D.L., and Angelides, K.J. (1989). Localization and mobility of omega-conotoxin-sensitive Ca^{2+} channels in hippocampal CA1 neurons. Science 244, 1189.

Jones, S.W., and Marks, T.N. (1989). Calcium currents in bullfrog sympathetic neurons. I. Activation kinetics and pharmacology. J. Gen. Physiol. 94, 151-167.

Kamiya, H., Sawada, S., and Yamamoto, C. (1988). Synthetic omega-conotoxin blocks synaptic transmission in the hippocampus in vitro. Neurosci. Lett. 91, 84-88.

Kasai, H. (1991). Tonic inhibition and rebound facilitation of a neuronal calcium channel by a GTP-binding protein. Proc. Natl.Acad. Sci. U.S.A. 88, 8855-8859.

Kasai, H., and Neher, E. (1992). Dihydropyridine-sensitive and omega-conotoxin-sensitive calcium channels in a mammalian neuroblastome-glioma cell line. J. Physiol. 448, 161-188.

Kass, R.S., and Sanguinetti, M.C. (1984). Inactivation of calcium current in the calf Purkinje fiber. Evidence for voltage- and calcium-mediated mechanisms. J. Gen. Physiol. 84, 705-726.

Kerr, L.M., Filloux, F., Olivera, B.M., Jackson, H, and Wamsley, J.K. (1988). Autoradiographic localization of calcium channels with [^{125}I]omega-conotoxin in rat brain. Eur. J. Pharmacol. 146, 181-183.

Kerr, L.M., and Yoshikami, D. (1984). A venom peptide with a novel presynaptic blocking action. Nature 308, 282-284.

Koch, W.J., Ellinor, P.T., and Schwartz, A. (1990). cDNA cloning of a dihydropyridine-sensitive calcium channel from rat aorta. J. Biol. Chem. 265, 17786-17791.

Kokubun, S. and Reuter, H. (1984). Dihydropyridine derivatives prolong the open state of Ca^{2+} channels in cultured cardiac cells. Proc. Natl. Acad. Sci. U.S.A. 81, 4824-4827.

Komuro, H., and Rakic, P. (1992). Selective role of N-type calcium channels in neuronal migration. Science 257, 806-809.

Lacerda, A.E., and Brown, A.M. (1989). Nonmodal gating of cardiac calcium channels as revealed by dihydropyridines. J. Gen. Physiol. 93, 1243-1273.

Leonard, J.P., Nargeot, J., Snutch, T.P., Davidson, N., and Lester, H.A. (1987). Ca channels induced in Xenopus oocytes by rat brain mRNA. J. Neurosci. 7, 875-881.

Levi., G., Aloisi, M., Ciotti, M., and Gallo, V. (1984). Autoradiographic localization and depolarization-induced release of amino acids in differentiating granule cells cultures. Brain Res. 290, 77-86.

Lin, J.W., Rudy, B., and Llinas, R.R. (1990). Funnel-web spider venom and a toxin fraction block calcium current expressed from rat brain mRNA in Xenopus oocytes. Proc. Natl. Acad. Sci. USA 87, 4538-4542.

Llinas, R.R., Sugimori, M, Lin, J.W., and Cherskey, B. (1989). Blocking and isolation of a calcium channel from neurons in mammals and cephalopods utilizing a toxin fraction (FTX) from funnel-web spider poison. Proc. Natl. Acad. Sci. USA 86, 1689-1693.

Maeda N., et al. (1989). Autoradiographic visualization of a calcium channel antagonist, omega-conotoxin GVIA, binding site in the brains of normal and cerebellar mutant mice (pcd and weaver). Brain Res. 489, 21-30.

Malaisse-Lagae, F.P., Mathias, C.F., and Malaisse, W.J. (1984). Gating and blocking of calcium channels by dihydropyridines in the pancreatic B-cells. Biochem. Biophys. Res. Commun. 123, 1062-1068.

Marchetti, C., Carignani, C., and Robello, M. (1991). Voltage-dependent calcium currents in dissociated granule cells from rat cerebellum. Neuroscience 43, 121-133.

McCleskey, E.W., Fox, A.P., Feldman, D.H., Cruz, L.J., Olivera, B.M., and Tsien R.W. (1987). Omega-conotoxin: Direct and persistent blockade of specific types of calcium channels in neurons but not in muslce. Proc. Natl. Acad. Sci. USA 84, 4327-4331.

McManus, O.B., Blatz, A.L., and Magleby, K.L. (1987). Sampling, log binning, fitting and plotting durations of open and shut intervals from single channels and the effect of noise. Pfluegers Arch 410, 530-553.

Mikami, A., Imoto, T., Tanabe, T., Niidome, T., Mori, Y., Takeshima, H., Naruniya, S., and Numa, S. (1989). Primary structure and functional expression of the cardiac dihydropyridine-sensitive calcium channel. Nature 340, 230-233.

Miller, R.J. (1987). Multiple calcium channels and neuronal function. Science 235, 46-52.

Miller, R.J. (1992). Voltage-sensitive calcium channels. J. Biol. Chem. 267, 1403-1406.

Mintz, I.M., Adams, M.E., and Bean, B.P. (1992a). P-type calcium channels in rat central and peripheral neurons. Neuron 9, 85-95.

Mintz, I.M., Venema, V.J., Swiderek, K.M., Lee, T.D., Bean, B.P., and Adams, M.E. (1992b). P-type calcium channels blocked by the spider toxin omega-Aga-IVA. Nature 355, 827-829.

Mogul, D.J., and Fox, A.P. (1991). Evidence for multiple types of Ca^{2+} channels in acutely isolated hippocampal CA3 neurones of the guinea-pig. J. Physiol. 433, 259-281.

Moran, O., Lin, F., Zegarra-Moran, O., and Sciancalepore, M. (1991). Voltage dependent calcium channels in cerebellar granule cell primary cultures. Eur. Biophys. J. 20, 157-164.

Mori, Y., Friedrich, T., Kim, M.S., Mikami, A., Nakai, J., Ruth, P., Bosse, E., Hofmann, F., Flockerzi, V., and Furuichi, T., Mikoshiba, K., Imoto, K., Tanabe, T., and Numa, S. (1991). Primary structure and functional expression from complementary DNA of a brain calcium channel. Nature 350, 398-402.

Murphy, T.H., Worley, P.F., and Baraban, J.M. (1991). L-type voltage-sensitive calcium channels mediate synaptic activation of immediate early genes. Neuron 7, 625-635.

Nowycky, M.C., Fox, A.P., and Tsien, R.W. (1985). Long-opening mode of gating of neuronal calcium channels and its promotion by the dihydropyridine calcium agonist Bay K 8644. Proc. Natl. Acad. Sci. U.S.A. 82, 2178-2182

Nowycky, M.C., Fox, A.P., and Tsien, R.W. (1985). Three types of neuronal calcium channel with different calcium agonist sensitivity. Nature 316, 440-443.

Perez-Reyes, E., Kim, H.S., Lacerda, A.E., Horne, W., Wei, X., Rampe, D., Campbell, K.P., Brown, A.M., and Birnbaumer, L. (1989). Induction of calcium currents by the expression of the α_1-subunit of the dihydropyridine receptor from skeletal muscle. Nature 340, 233-236.

Perez-Reyes, E., Wei, X., Castellano, A., and Birnbaumer, L. (1990). Molecular diversity of L-type calcium channels. J. Biol. Chem. 265, 20430-20436.

Perney, T.M., Hirning, L.D., Leeman, S.E., and Miller, R.J. (1986). Multiple calcium channels mediate neurotransmitter release from peripheral neurons. Proc. Natl. Acad. Sci. USA 83, 6656-6659.

Pietrobon, D., Di Virgilio, F., and Pozzan, T. (1990). Structural and functional aspects of calcium homeostasis in eukaryiotic cells. Eur. J. Biochem. 193, 599-622.

Pietrobon, D., Calderini, G., and Forti, L. (1991). Calcium channels in rat cerebellar neurons. Soc. Neurosci. Abstr. 17, 342.

Pietrobon, D., and Hess, P. (1990). Novel mechanism of voltage-dependent gating in L-type calcium channels. Nature 346, 651-655.

Plummer, M.R., and Hess, P. (1991). Reversible uncoupling of inactivation in N-type calcium channels. Nature 351, 657-659.

Plummer, M.R., Logothetis, D.E., and Hess, P. (1989). Elementary properties and pharmacological sensitivities of calcium channels in mammalian peripheral neurons. Neuron 2, 1453-1463.

Rane, S.G., Holz, G.G. IV, and Dunlap, K. (1987). Dihydropyridine inhibition of neuronal calcium current and substance P release. Pfluegers Arch. 409, 361-366.

Rao, C,R. (1973). Linear statistical inference and its applications. John Wiley, New York.

Reisine, T. (1990). Cellular mechanism of somatostatin inhibition of calcium influx in the anterior pituitary cell line AtT-20. J. Pharmacol. Exp. Ther. 254, 646-651.

Regan, L.J., Sah, D.W.Y., and Bean, B.P. (1991). Ca^{2+} channels in rat central and peripheral neurons: high-threshold current resistant to dihydropyridine blockers and -Conotoxin. Neuron 6, 269-280.

Regulla, S., Schneider, T., Nastainczyk, W., Meyer, H.E., and Hoffmann, F. (1991). Identification of the site of interaction of the dihydropyridine channel blockers nitrendipine and azidopine with the calcium-channel α_1 subunit. EMBO J. 10, 45-49.

Reuter, H., Stevens, C.F., Tsien, R.W., and Yellen, G. (1982). Properties of single calcium channels in cardiac cell culture. Nature 297, 501-504.

Robitaille, R., Adler, E.M., and Charlton, M.P. (1990). Strategic location of calcium channels at transmitter sites of frog neuromuscular synapses. Neuron 5, 773-779.

Ruth, P., Rohrkasten, A., Biel, M., Bosse, E., Regulla, S., Meyer, H.E., Flockerzi, V., and Hoffmann, F. (1989). Primary structure of the ß subunit of the DHP-sensitive calcium channel from skeletal muscle. Science 245, 1115-1118.

Sanguinetti, M.C., and Kass, R.S. (1984). Voltage-dependent block of calcium channel current in the calf Purkinje fiber by dihydropyridine calcium channel antagonists. Circ. Res. 55, 336-348.

Schroeder, J.E., Fischbach, P.S., Mamo, M., and McCleskey, E.W.(1990). Two components of high-threshold Ca^{2+} current inactivate by different mechanisms.

Neuron 5, 445-452.

Sciancalepore, M., Forti, L., and Moran, O. (1989). Changes of N-methyl-D-aspartate activated channels of cerebellar granule cells with days in culture. Biochem. Biophys. Res. Comm. 165, 481-487.

Seabrook, G.R., and Adams, D.J. (1989). Inhibition of neurally-evoked transmitter release by calcium channel antagonists in rat parasympathetic ganglia. Br. J. Pharmacol. 97, 1125-1136.

Sigworth, F.J., and Sine, S.M. (1987). Data transformation for improved display and fitting of single-channel dwell time histograms. Biophys. J. 52, 1047-1054.

Slesinger, P.A., and Lansman, J.B. (1991a). Reopening of Ca^{2+} channels in mouse cerebellar neurons at resting membrane potentials during recovery from inactivation. Neuron 7, 755-762.

Slesinger, P.A., and Lansman, J.B. (1991b). Inactivating and non-inactivating dihydropyridine-sensitive Ca^{2+} channels in cerebellar granule cells. J. Physiol. 439, 301-323.

Snutch, T.P., Leonard, J.P., Gilbert, M.M., Lester, H.A., and Davidson, N. (1990). Rat brain expresses a heterogeneous family of calcium channels. Proc. Natl. Acad. Sci. USA 87, 3391-3395.

Snutch, T.P., Tomlinson, W.J., Leonard, J.P., and Gilbert, M.M. (1991). Distinct calcium channels are generated by alternative splicing and are differentially expressed in the mammalian CNS. Neuron 7, 45-57.

Snutch, T.P. and Reiner, P.B. (1992). Ca^{2+} channels: diversity of form and function. Curr. Opin. Neurobio. 2, 247-253.

Takahashi, M., Seager, M.J., Jones, J.F., Reber, B.F.X., and Catterall, W.A. (1987). Subunit structure of dihydropyridine-sensitive brain calcium channels. Proc. Natl. Acad. Sci. USA 84, 5478-5482.

Takemura, M., Kiyama, H., Fukui, H., Toyama, M., and Wada, H. (1988). Autoradiographic visualization in rat brain of receptors for omega-conotoxin GVIA, a newly discovered calcium antagonist. Brain Res. 451, 386-389.

Tanabe, T., Takeshima, H., Mikami, A., Flockerzi, V., Takahashi, H., Kangawa, K., Kojima, M., Matsuo, H., Hirose, T., Numa, S. (1987). Primary structure of the receptor for calcium channel blockers from skeletal muscle. Nature 328, 313-318.

Tanabe, T., Beam, K.G., Adams, B.A., Niidome, T., and Numa, S. (1990). Regions

of the skeletal muscle dihydropyridine receptor critical for excitation-contraction coupling. Nature 346, 567-569.

Torri-Tarelli, F., Passafaro, M., Clementi, F., and Sher, E. (1991). Presynaptic localization of omega-conotoxin-sensitive calcium channels at the frog neuromuscular junction. Brain Res.547, 331-334.

Tsien, R.W., Lipscombe, D., Madison, D.V., Bley, K.R., and Fox, A.P. (1988) Multiple types of neuronal calcium channels and their selective modulators. Trends Neurosci. 11, 431-438.

Tsien, R.W., Ellinor, P.T. and Horne W.A. (1991). Molecular diversity of voltage-dependent Ca^{2+} channels. Trends Pharmacol.Sci. 12, 349-354.

Uchitel, O., Protti, D.A., Sanchez, V., Cherskey, B.D., Sugimori, M., and Llinas, R.R.(1992).P-type voltage-dependent caclium channel mediates presynaptic calcium influx and transmitter release in mammalian synapses. Proc. Natl. Acad. Sci. USA 89, 3330-3333.

Usowicz, M.M., Sugimori, M., and Llinas, R. (1991). Elementary properties of calcium channels in cerebellar Purkinje neurons. Soc. Neurosc. Abstr. 17, 342.

Wagner, J.A., Snowman, A.M., Biswas, A., Olivera, B.M., and Snyder, S.H. (1988). Omega-conotoxin GVIA binding to a high-affinity receptor in brain: characterization, calcium sensitivity, and solubilization. J. Neurosci. 8, 3354-3359.

Wickens, J.R., and Abraham, W.C. (1991). The involvement of L-type calcium channels in heterosynaptic long-term depression in the hippocampus. Neurosci. Lett. 130, 128-132.

Williams, M.E., Feldman, D.H., McCue, A.F., Brenner, R., Velicelebi, G., Ellis, S.B., and Harpold, M.M. (1992a). Structure and functional expression of α_1, α_2, and ß subunits of a novel human neuronal calcium channel subtype. Neuron 8, 71-84.

Williams, M.E., Brust, P.F., Feldman, D.H., Patthi, S., Simerson, S., Maroufi, A., McCue, A.F., Velicelebi, G., Ellis, S.B., and Harpold, M.M. (1992b). Structure and functional expression of an omega-conotoxin-sensitive human N-type channel. Science 257, 389-395.

Yue, D.T., Herzig, S., and Marban, E. (1990). ß-adrenergic stimulation of calcium channels occurs by potentiation of high activity gating modes. Proc. Natl. Acad. Sci. U.S.A. 87, 753-757.

Acknowledgments

I would like to thank Prof. Daniela Pietrobon for giving me the opportunity to perform this work and for her careful supervision. I am indebted to Dr. Steve Skaper of Fidia Research Laboratories for kind help with cell cultures, with Dr. Siro Luvisetto and Dr. Angelita Tottene for much help in the laboratory, with Dr. M. Zoratti, Dr. M. Murgia, Dr. B.P. Bean, Prof. C. Montecucco and Prof. T. Pozzan for reading parts of this manuscript.
This work was performed at the Department of Biomedical Sciences of the University of Padova. I was finacially supported by the International School for Advanced Studies (Trieste) and by Fidia (Abano Terme, Padova), whom I thank. I am indebted to Prof. G.F. Azzone, Prof. D. Amati and Prof. E. Cherubini for providing me support to pursue this work.